

Accepted Manuscript

The Ionian and Alfeo-Etna fault zones: New segments of an evolving plate boundary in the central Mediterranean Sea?

A. Polonia, L. Torelli, A. Artoni, M. Carlini, C. Faccenna, L. Ferranti, L. Gasperini, R. Govers, D. Klaeschen, C. Monaco, G. Neri, N. Nijholt, B. Orecchio, R. Wortel

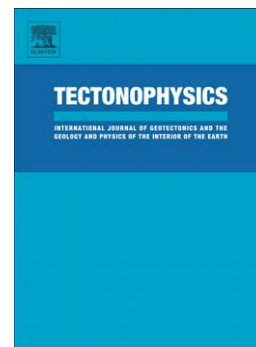
PII: S0040-1951(16)30009-9
DOI: doi: [10.1016/j.tecto.2016.03.016](https://doi.org/10.1016/j.tecto.2016.03.016)
Reference: TECTO 127008

To appear in: *Tectonophysics*

Received date: 13 October 2015
Revised date: 10 March 2016
Accepted date: 14 March 2016

Please cite this article as: Polonia, A., Torelli, L., Artoni, A., Carlini, M., Faccenna, C., Ferranti, L., Gasperini, L., Govers, R., Klaeschen, D., Monaco, C., Neri, G., Nijholt, N., Orecchio, B., Wortel, R., The Ionian and Alfeo-Etna fault zones: New segments of an evolving plate boundary in the central Mediterranean Sea?, *Tectonophysics* (2016), doi: [10.1016/j.tecto.2016.03.016](https://doi.org/10.1016/j.tecto.2016.03.016)

This is a PDF file of an unedited manuscript that has been accepted for publication. As a service to our customers we are providing this early version of the manuscript. The manuscript will undergo copyediting, typesetting, and review of the resulting proof before it is published in its final form. Please note that during the production process errors may be discovered which could affect the content, and all legal disclaimers that apply to the journal pertain.



THE IONIAN AND ALFEO-ETNA FAULT ZONES: NEW SEGMENTS OF AN EVOLVING PLATE BOUNDARY IN THE CENTRAL MEDITERRANEAN SEA?

Polonia A.¹, Torelli L.², Artoni A.², M. Carlini², Faccenna C.³, Ferranti L.⁴, Gasperini L.¹, Govers R.⁵, Klaeschen D.⁶, Monaco C.⁷, Neri G.⁸, Nijholt N.⁵, Orecchio B.⁸, Wortel R.⁵

1- Institute of Marine Science CNR ISMAR-Bo, Via Gobetti, 101, 40129 Bologna, Italy
Tel: +39 051-6398888, e-mail: alina.polonia@ismar.cnr.it

2- Department of Physics and Earth Sciences, University of Parma, Parco Area delle Scienze, 157/A – Parma

3-Laboratory Experimental Tectonics, Dipartimento Scienze - Università Roma TRE, Largo S.L.Murialdo 1 - Roma

4- Department of Earth Sciences, Environment and Resources, Univ. of Napoli "Federico II", Largo S. Marcellino 10, Napoli.

5- Department of Earth Sciences, Utrecht University, P.O. Box 80.115, 3508 TC Utrecht, Netherlands

6- GEOMAR Helmholtz Centre for Ocean Research Kiel Kiel, Germany

7- Department of Biological, Earth and environmental sciences, University of Catania, Corso Italia, 57 Catania

8- Department of Physics and Earth Sciences, University of Messina, Viale F. Stagno d'Alcontres 31, Messina, Italy.

Abstract

The Calabrian Arc is a narrow subduction-rollback system resulting from Africa/Eurasia plate convergence. While crustal shortening is taken up in the accretionary wedge, transtensive deformation accounts for margin segmentation along transverse lithospheric faults. One of these structures is the NNW-SSE transtensive fault system connecting the Alfeo seamount and the Etna volcano (Alfeo-Etna Fault, AEF). A second, NW-SE crustal discontinuity, the Ionian Fault (IF), separates two lobes of the CA subduction complex (Western and Eastern Lobes) and impinges on the Sicilian coasts south of the Messina Straits.

Analysis of multichannel seismic reflection profiles shows that: 1) the IF and the AEF are transfer crustal tectonic features bounding a complex deformation zone, which produces the downthrown of the Western lobe along a set of transtensive fault strands; 2) during Pleistocene times, transtensive faulting reactivated structural boundaries inherited from the Mesozoic

Tethyan domain which acted as thrust faults during the Messinian and Pliocene; 3) the IF and the AEF, and locally the Malta escarpment, accommodate a recent tectonic event coeval and possibly linked to the Mt. Etna formation.

Regional geodynamic models show that, whereas AEF and IF are neighboring fault systems, their individual roles are different. Faulting primarily resulting from the ESE retreat of the Ionian slab is expressed in the northwestern part of the IF. The AEF, on the other hand, is part of the overall dextral shear deformation, resulting from differences in Africa-Eurasia motion between the western and eastern sectors of the Tyrrhenian margin of northern Sicily, and accommodating diverging motions in the adjacent compartments, which results in rifting processes within the Western Lobe of the Calabrian Arc accretionary wedge. As such, it is primarily associated with Africa-Eurasia relative motion.

1.0 – Introduction

The Calabrian Arc (CA) (Figure 1) is a narrow and arcuate subduction-rollback system related to the Africa/Eurasia plate convergence and the southeastward retreat of the Tethyan slab (Rehault et al., 1984; Malinverno and Ryan, 1986; Gueguen et al., 1998; Jolivet and Faccenna, 2000; Faccenna et al., 2001a, 2004; Rosenbaum and Lister, 2004). Back-arc extension in the Liguro-Provençal Basin since ~ 30 Ma, and in the Tyrrhenian Sea since ~10 Ma (Malinverno and Ryan, 1986; Patacca et al., 1990; Gueguen et al., 1998; Faccenna et al., 2001b; Rosenbaum et al., 2002; Nicolosi et al., 2006) accommodated 1200 km of displacement of Calabria to its present position (Bonardi et al., 2001; Faccenna et al., 2001a; Barberi et al., 2004; Rosenbaum and Lister, 2004).

Tomographic images in the central CA show a continuous slab penetrating into the mantle (Bijwaard and Spakman, 2000; Wortel and Spalman, 2000; Faccenna et al., 2007; Neri et al., 2009;

2012) and a well defined Wadati-Benioff zone (Wortel and Spakman, 2000) is marked by earthquakes down to nearly 500 km depth (Selvaggi and Chiarabba, 1995). In this area, geodetic measurements suggest the outward motion of Calabria relative to Apulia (GPS rate of 2 mm/yr, D'Agostino et al., 2008) with shortening accommodated in the accretionary wedge (Polonia et al., 2011). Furthermore, tomographic imaging has shown that the deep (lithosphere-upper mantle) structure in the Calabrian-Sicily region has the characteristics of a STEP setting, similar to that of the northern Tonga subduction zone (Carminati et al., 1998; Wortel et al., 2009). The Calabria slab has distinct edges and a Subduction-Transform Edge Propagator (STEP, Govers and Wortel, 2005) laterally bounds the narrow CA in both the northeast and southwest. These are loci of lithospheric tearing that result from the subduction of the (retreating) Calabria slab while adjacent parts (Apulia, Sicily) remain at the earth surface. The plate boundary between the overriding plate and the surface plate that develops in the wake of the STEP is referred to as the "STEP fault" (Baes et al., 2011). The geometry and kinematics of a STEP fault (or fault zone [Özbakır et al., 2013]) are still poorly constrained, on the one hand because of their dependence on the regional situation, presumably resulting in a great variety of expressions and, on the other hand, owing to the lack of direct, diagnostic observations, as exemplified by incomplete (too short) records of earthquake activity accompanying STEP action.

Geodetic data highlight the presence of distinct deformation belts separating the Tyrrhenian Sea, and the Sicily and Calabria blocks, which interfere in NE Sicily and the Messina Straits area (Palano et al., 2012; Doglioni et al., 2012; D'Agostino and Selvaggi, 2004; Serpelloni et al., 2005). Several regional-scale active structures were proposed in this region: the southern Tyrrhenian contractional belt, along which tectonic inversion occurred since the middle Pleistocene (see also Pepe et al., 2005; Billi et al., 2007, 2011); the Aeolian-Tindari fault system, whose southward continuation into the Ionian offshore is controversial (Billi et al., 2006); the Messina fault, whose

strike and pitch are also not completely agreed upon (Amoruso et al., 2002; Aloisi et al., 2012; Doglioni et al., 2012), and the Cefalù-Etna tectonic boundary (Billi et al., 2010). This complex setting was commonly related to a Middle Pleistocene tectonic reorganization in the southern-central Mediterranean driven by the stalling of the Calabrian roll-back/subduction and related Tyrrhenian back-arc extension (Wortel and Spakman, 2000; Goes et al., 2004; Faccenna et al., 2011). This process probably resulted in several crustal expressions, including the partial jump of the Sicilian thrusting towards the southern Tyrrhenian contractional belt, the increased extension and uplift rates in W Calabria and NE Sicily, the variation in chemical composition of magmas in the eastern Aeolian arc (De Astis et al., 2000), and the triggering of Mt. Etna volcanism (Gvirtzman and Nur, 1999; Doglioni et al., 2001; Faccenna et al., 2011).

GPS and seismicity observations suggest that the subducting African plate may contain several active fault/shear zones (Oldow et al., 2002; D'Agostino et al., 2008). Apulia may be moving with the Ionian Sea and the Hyblean Plateau, while Adria has a distinctly different motion (D'Agostino et al., 2008). In this framework, a key question is the role played by the submerged CA and the Ionian domain, which is described either as part of the Hyblean-Malta block or as part of the diverging Apulian block moving towards the northeast, relative to Europe (Palano et al., 2012). The presence of transtensional and normal faults in the Eastern Sicily offshore (Nicolich et al., 2000; Chamot-Rooke et al., 2005) suggests that the small geodetic divergence of the Hyblean and Apulian blocks is in agreement with a deep fragmentation of the Ionian domain (Palano et al., 2012). However, the relative motion of these blocks cannot be constrained due to the lack of geodetic observations at sea.

Starting from this background, the aim of this study is to unravel the geometry and nature of the complex plate boundary segment in the study area. We first summarize results obtained from previous studies (section 2.0) on the overall structure of the submerged subduction complex

(Figures 2 and 3). Then, we present four newly re-processed Multi-Channel Seismic (MCS) lines collected parallel to the trench (Figures 4-8) that enable us to highlight along-strike tectonically active features. Activity of such faults is discussed through the analysis of high resolution single channel seismic profiles (Chirp and Sparker lines in Figures 4 and 9) and multibeam data. Finally, we combine the structural information from marine seismic data with seismological data (on seismicity and upper mantle structure) and numerical modelling to arrive at a model for terminal stage subduction in the CA and the accompanying plate boundary evolution. Through our integrated approach, we investigate the geodynamic significance of the major fault systems, their depth-surface relationships and their evolution in terms of lithosphere dynamics, including the hypothesis they may represent STEP faults. The results of our analysis support margin segmentation in the central Mediterranean Sea involving lithospheric structures inherited from the Mesozoic Tethyan Ocean, which accommodate slab tearing processes and relative plate motion.

2.0– The Calabrian Arc: subduction complex and regional context

2.1 – Crustal tectonics near Sicily

The southern Tyrrhenian area is fragmented into crustal blocks separated by seismically active belts (Palano et al., 2012 and references therein). Contraction affects mainly the western sector of the Southern Tyrrhenian Sea (Figure 1) where focal mechanism solutions indicate the presence of an E-W oriented compressive belt, which extends from the Aeolian archipelago to the Ustica Island (Neri et al., 2005; Billi et al., 2006, 2007, 2010). This is characterized by 1–1.5 mm/yr of geodetic shortening (Serpelloni et al., 2005; Devoti et al., 2011; Palano et al., 2012) and by frequent, moderate-sized crustal (15–20 km of depth) thrust earthquakes (Pondrelli et al., 2006; Billi et al., 2007; Giunta et al., 2009), with P axes constantly trending NW–SE. The earthquake distribution of single seismic sequences pointed out that the seismically active contractional

structures are high-angle, N-dipping, segmented, reverse faults (10-20 km in length) (Billi *et al.*, 2007). The steep orientation of these faults can be due to the reactivation of normal faults (Pepe *et al.*, 2005). Focal mechanisms indicate a purely reverse mechanism with a NNW-SSE oriented P axis (Billi, *et al.*, 2007; Pondrelli *et al.*, 2006). Geodetic, seismological and geological data (Monaco *et al.*, 1996; Lavecchia *et al.*, 2007; Mattia *et al.*, 2012; Barreca *et al.*, 2014a; De Guidi *et al.*, 2015) indicate that Nubia-Eurasia convergence is also accommodated by active thrusting and folding across the Sicily chain front (up to 4.5 mm/yr of geodetic shortening).

Conversely, the eastern sector (NE Sicily and W Calabria) is dominated by late Quaternary extension (Monaco and Tortorici, 2000; Jacques *et al.*, 2001; Ferranti *et al.*, 2008; Scarfi *et al.*, 2009). This implies the presence of a transition zone between these two belts, which is tentatively placed along a transversal NNW-SSE oriented tectonic boundary (the Aeolian-Tindari-Letojanni fault system of Palano *et al.* (2012)) (Figure 1).

As suggested by geological, geodetic and seismological data (Cuppari *et al.*, 1999; De Astis *et al.*, 2003; Goes *et al.*, 2004; Favalli *et al.*, 2005; Neri *et al.*, 2005; Govers and Wortel, 2005; Billi *et al.*, 2006; Mattia *et al.*, 2008; Palano *et al.*, 2012; De Guidi *et al.*, 2013; Scarfi *et al.*, 2013), this regional discontinuity in the Tyrrhenian offshore, is characterized by transtensional right-lateral motion. It appears to have a primary role in the geodynamics of the Aeolian sector of the southern Tyrrhenian domain, influencing both seismicity and volcanism (Barreca *et al.*, 2014b). Active dextral transtension along the NNW-striking branch of this fault system in NE Sicily across the Peloritani Mts. (Figure 1) has been described on-land up to the Novara village (Billi *et al.*, 2006; De Guidi *et al.*, 2013). This fault system has been further defined through geodetic and seismological studies (Neri *et al.*, 2005; Mattia *et al.*, 2008). In particular, it is characterized by GPS relative velocities of ~ 3.6 mm/yr along the N126E direction (Mattia *et al.*, 2009; Palano *et al.*, 2012), and by an alignment of deep earthquakes (Scarfi *et al.*, 2005, 2013). Despite the lack of clear field

evidence (Billi et al., 2006), several authors proposed that this active fault system in the Southern Tyrrhenian Sea continued to the Ionian coast of Sicily north of Mt. Etna (e.g., Govers and Wortel, 2005 and references therein; Rosenbaum et al., 2008).

In addition to the Aeolian-Tindari fault system, CMT solutions, GPS data and structural geology show active extension along an incipient fault zone extending from Mt. Etna to Cefalù along WNW-ENE trends (Neri et al., 2005; Billi et al., 2006, 2010; Devoti et al., 2011; Palano et al., 2012). Although Lavecchia et al. (2007) interpreted this incipient extension as ensuing from upper crustal stretching above an active thrust belt, Billi et al. (2010) favor reactivation of pre-existing faults and upwelling of melt mantle material beneath Mount Etna. A better understanding of active faults in the Ionian Sea is thus crucial to define if upper plate fault systems are controlled by structural development in the offshore region and which are the regional processes driving recent plate-boundary re-organization.

2.2 - The CA subduction complex

The Africa/Eurasia plate convergence and slab rollback in the Tyrrhenian/Calabrian region generated a 10-30 km thick, 300 km wide subduction system, which encompasses a sub-aerial complex constituted by crystalline rocks and Meso-Cenozoic sedimentary units (Amodio-Morelli et al., 1976) overlaid by a submarine accretionary wedge (Cernobori et al., 1996; Doglioni et al., 1999; Minelli and Faccenna, 2010; Polonia et al., 2011; Gallais et al., 2012).

The emplacement of the accretionary wedge is related to offscraping and underplating of the thick sedimentary section resting on the lower African plate and shortening is taken up along the outer deformation front and in the inner portions of the accretionary wedge.

Three main morpho-structural domains were identified within the subduction complex (Polonia et al., 2011). From SE to NW they are: i) the frontal salt-bearing post-Messinian

accretionary wedge (yellow areas in Figures 2 and 3); ii) the pre-Messinian clastic accretionary wedge (green area in Figures 2 and 3); and iii) the inner plateau, a morphologically flat sector where forearc basins develop on top of the continental basement (Figure 3b). Variations of structural style and seafloor morphologies in these domains are related to changes in sediment rheology and different tectonic processes. The emplacement of the Messinian evaporites in the subducting sedimentary section caused an abrupt change in wedge build-up processes, reflected in variations of topographic slope angles, basal detachment depths, structural style and a very high velocity of outward movement of the outer deformation front. The post-Messinian accretionary wedge is made primarily of evaporites and frontal accretion does actually occur in this domain, along a basal detachment located at the base of the Messinian evaporites. Tertiary and Mesozoic sediments constitute the pre-Messinian accretionary wedge, where the basal detachment cuts through deeper levels. The transition between the pre-Messinian accretionary wedges and the flat inner plateau is marked by complex fault systems, which favour fluid migration and mud volcanism (Panieri et al., 2013).

The accretionary complex is segmented across strike by crustal transfer tectonic systems representing the shallow expression of deeply rooted processes. In the following sub-section, we summarize the geometry and kinematics of these fault systems deduced from previous studies (Polonia et al., 2011, 2012).

2.3 – Segmentation of the subduction complex in the Ionian Sea

First order margin segmentation occurs along a NW-SE trending deformation belt delimiting two distinct lobes of the subduction complex (Figure 2). This deformation zone runs from the Messina Straits region to the Ionian abyssal plain, dissecting the entire subduction complex. In the Eastern Sicily offshore, the Western Lobe (WL) is constituted by a very low (about 1.5°) tapered

salt-bearing accretionary wedge (Figures 2 and 3a), bounded towards the continent by a slope terrace, where a Messinian thrust-top basin develops. This flat region is located where the basal detachment, located along the base of the Messinian evaporites, cuts through deeper reflectors down to the basement, involving the formation of out of sequence thrusts (splay faults) and duplexes (Figure 2). The Eastern Lobe (EL), in front of Central Calabria, shows a completely different structure, characterized by a more elevated accretionary wedge, 1000-1500 m shallower than in the WL, steeper topographic slopes, and higher deformation rates (Figures 2 and 3b). The Eastern lobe is not fronted by an undeformed abyssal plain since it already collided with the Mediterranean Ridge. Structural style variation between the two lobes corresponds to differences in the basal detachment depth (about 4 Km shallower in the western lobe) and to the presence of thrust faults involving the basement in the eastern lobe (Figure 3b).

In the WL, across strike margin segmentation is more diffuse, and develops along a set of NNW-SSE trending fault systems (Hirn et al., 1997; Bianca et al., 1999; Nicolich et al., 2000; Chamot-Rooke et al., 2005; Argnani and Bonazzi, 2005; Del Ben et al., 2008; Rosenbaum et al., 2008; Polonia et al., 2011, 2012; Gallais et al., 2013). The main fault strand is represented by an active transtensive structure running from the Alfeo seamount to the offshore of the Mt. Etna volcano. This system of normal faults re-activates a Messinian/Pliocene thrust fault, and produces a vertical displacement of the accretionary wedge down to the deepest reflectors (Figure 3c). It develops along an inherited Mesozoic discontinuity marked by a sedimentary basin filled by a thick (up to 700 m) and relatively undeformed sedimentary sequence (Polonia et al., 2011, 2012).

In this study, the tectonic boundary displacing two lobes of the CA accretionary wedge is named *Ionian Fault* (IF), because it runs through the entire CA subduction complex in the Ionian Sea. Furthermore, the NNW-SSE trending fault in the Western lobe is named *Alfeo-Etna Fault System* (AEF), to underline that it connects the Alfeo seamount and the Etna volcano offshore.

3.0 – New constraints on wedge structures

3.1– Analysis of new seismic data in the Ionian Sea

A relatively close-spaced grid of seismic reflection data was re-processed and interpreted to define geometry and deformation pattern of the IF and the AEF. We present here four multichannel seismic lines (MCS) across the two fault systems from the Messina Straits to the Southern Ionian Sea (Figure 4).

We used all available seismic datasets (the CNR_ENI Deep Crust Seismic Profiles – CROP, the ENI CA MCS seismic, the high resolution MCS CALAMARE lines, the sparker J dataset and Chirp profiles), characterized by different vertical resolutions (Table 1), to describe geometry and kinematics of the fault systems segmenting the western Ionian Sea. Multibeam data integrate deep seismic data and constrain the fine structure of the fault systems. Seismic data specification and resolution of each data set are reported in Table 1.

3.1.1 - Seismic line CROP C92-31

Seismic profile C92-31 of the CROP data-set (Figure 5) was collected to the S of the Messina Straits in the Ionian Sea (see Figure 4 for location). The complex tectonic setting of this region is outlined by the close-spaced alternation of distinct structural domains characterized by varying deformation patterns. Deep deformation is associated with oppositely verging thrust faults in the central part of the seismic line, where a 1.5 sec TWT thick well-stratified and a relatively undeformed sedimentary section, slightly dipping towards the W is present (s.p. 1100-1300 Figure 5). This basin may be described as a pop-down related to west-dipping thrust faults to the west and east-dipping thrust fault to the east. A sub-vertical fault slightly dipping to the West is present

on the western margin of such basin (s.p. 1120 in Figure 5) and it marks the abrupt transition between the undeformed sediments to the W and folded sediment packets to the East.

Between s.p. 1300 and 1400 a major west-dipping fault is imaged on the seismic section where a canyon system is also present. Disruption of sediment layering and the presence of westward dipping reflectors suggest it is a sub-vertical strike slip fault affecting seismic reflectors from the seafloor (Figure 5a) down to a depth of at least 6 sec TWT.

Three main sedimentary units were identified through stratigraphic correlation of seismic reflectors and available log data (Polonia et al., 2012). Recent sedimentation is represented by two distinct units of well-layered Plio-Quaternary deposits (Figure 5) separated by an angular middle-late Pliocene unconformity which acts as a detachment for slumping processes. Messinian sediments were deposited in two distinct basins separated by a structural high (s.p. 1500-1600). The geometry of seismic reflectors suggests that the basins were inverted by a compressive phase during mid-late Pliocene, as testified by the angular unconformity within the Plio-Quaternary sediments. Below the Messinian deposits, the brown unit represents upper Oligocene-upper Miocene sedimentary sequences, made of turbidite deposits unconformably laying over Peloritani-Aspromonte basement units, which appear to be highly deformed along oppositely verging thrust faults.

The geometry of seismostratigraphic units and their boundaries records the effects of four main tectonic phases starting from the Oligocene: i) an Oligocene shortening phase, pre-dating the deposition of the Oligocene-late Miocene clastic sedimentary units (brown unit in Figure 5); ii) a late Miocene localized extensional phase coeval to accretion processes; iii) a post-Messinian shortening, lasting up to the middle-late Pliocene (inverted Messinian basins), which produced the angular unconformity visible in the Plio-Quaternary sediments; iv) a lower Pleistocene extension, represented by transtensive faults on both sides of seismic line C92-31 (Figure 5).

The sub-vertical transtensive faults at s.p. 1100 and 1400 (Figure 5) belong to the IF system, which appears to re-activate the leading edge of pre-existing Pliocene thrust faults.

3.1.2 - Seismic line CA99-215

Seismic profile CA99-215 was collected in a SSW-NNE direction roughly parallel to the Calabria coast (Table 1 and Figure 4). The seismic profile shows a more elevated region offshore Calabria, while to the SSW, close to the Messina Straits area, a set of transtensive faults displace seismic reflectors and correspond to seafloor breaks and sub-vertical planes (Figure 6). The complex set of faults evidenced from s.p. 100 to s.p. 1500 merge in two main fault systems down to about 11 sec (TWT) which are associated with a basement offset. The basement represents the basal detachment of the pre-Messinian accretionary wedge.

3.1.3 - Seismic line CALA-02

Seismic line CALA-02 (Figure 7) was collected parallel to the trench axis in the region N of the Alfeo seamount (see Figure 4 for location). It runs between the Malta escarpment to the West, and the IF to the East (Figure 7), crossing the whole WL.

To the West, the deformed sediments of the accretionary wedge rest on the Mesozoic carbonates of the Malta escarpment dipping towards East. Here, the accretionary wedge is facing the Malta escarpment and is sealed by Plio-Quaternary sediments implying that frontal accretion does not actually occur in this region although shortening is taken up in the accretionary wedge. The AEF is clearly imaged close to s.p. 1850, where it displaces vertically the entire sedimentary sequence, and controls the formation of a sedimentary basin (Figure 7).

Towards East, the accretionary wedge is affected by a number of normal faults, which produce small scarps at the seafloor, throws of the recent sediments, and small troughs. A major

sedimentary basin is imaged on the easternmost part of the CALA 02 profile (sp. 600-400), where it is associated to a rather flat seafloor and a basement slightly dipping towards East, whose geometry is controlled by a system of normal faults dipping towards W (s.p. 500 and 230). This fault system is active as testified by the recent sedimentary basin and corresponds to the IF. Chirp profile in Figure 7c collected along the MCS seismic profile shows the set of normal faults controlling the sedimentary basin. The basin infill is rather transparent and uniform as it is constituted by coarse grained, loose sand sampled during the CALAMARE Urania cruise (core CALA 18 in Fig 7c).

3.1.4 - Seismic line CROP M-3

The deep-penetrating seismic line CROP M-3 (Figure 8) was acquired roughly parallel to the trench axis (see Figure 4 for location). It crosses the continental margin in a flat area corresponding to the mid-slope terrace, developing at the transition between the outer and the inner wedge (Figures 2 and 3). Four main morphotectonic domains are visible in the seismic section (Figure 8). To the West, the Malta escarpment is affected by deep normal faulting. However, recent undeformed sediments onlapping the steep slope suggest that this system is presently inactive in this sector. At the toe of the Malta escarpment, the salt-bearing accretionary wedge is represented by the orange unit (Figure 8), i.e., the post-Messinian accretionary complex detaching at the base of the evaporites. The wedge is sealed by Plio-Quaternary sediments, implying that in this region accretion was inactivated during Pliocene times, in agreement to what was observed in profile CALA-02 (see previous section). The green unit in Figure 8 corresponds to the heavily deformed pre-Messinian accretionary wedge made of Mesozoic carbonates and post-Aptian clastic sediments. The Eastern part of the seismic section runs over the EL of the subduction complex, which is again mainly constituted by evaporites (orange unit).

Structural boundaries between these domains are evidenced by eastward and westward dipping seismic reflectors, abrupt lateral changes of seismic facies, disruption of deep reflectors, correlating well with shallow morphological features (alignment of sedimentary basins, folds and seafloor notches).

The AEF corresponds to the boundary between the salt bearing wedge to the West, and the clastic pre-Messinian accretionary complex in the central part of the seismic line. This observation suggests that this fault re-activates the splay-1 (out-of sequence) thrust fault (Figures 2 and 3), which represents the deformation front of the CA subduction complex during the Messinian. At depth, it corresponds with a pre-existing Mesozoic crustal discontinuity, along which the basement is vertically displaced by over 1000 m.

The IF system at s.p. 3900, is marked by a deformation zone between the two lobes of the accretionary wedge and, similarly to the AEF, represents the transition between the pre and post-Messinian accretionary wedges (Figure 8) implying it was already in existence during late Miocene. In fact, it corresponds to a lateral ramp of the accretionary wedge, which was active during the Messinian. The westward dipping thrust fault imaged at s.p. 4800-4900 represents a recent compressive deformation front of the EL.

3.1.5 – High resolution single-channel seismic data

The tectonic activity of some of the fault systems was addressed through the analysis of single channel Chirp and Sparker seismic lines (Figure 9). Sparker seismic line in Figure 9a, highlights the presence of a fan shaped sedimentary basin developing above a major normal fault. This fault impinges along the coasts of Sicily north of the Mt. Etna where Chiocci et al. (2011) describe the northern bounding fault.

A Chirp profile collected on the opposite side of the entrance of the Messina Straits across the IF system shows (Figure 9b) a set of two normal faults offsetting the seafloor. At the toe of the fault three stacked submarine landslides are present suggesting sediment remobilization likely triggered by fault movement.

Chirp seismic line CQ14_174 (Figure 9c) collected across the IF system shows two oppositely dipping steep scarps along which the seafloor is downthrown of about 80 and 50 m. The depressed area marks the transition between a more coherent, highly reflective and high amplitude sediment assemblage to the East and a less reflective and rough seafloor to the West suggesting that the fault limbs are characterized by different lithologies (strike slip movement). The zoom of the Chirp profile shows active faulting on the seafloor on the eastern fault block.

Chirp profile in Figure 9d shows a fan shaped basin developing at the toe of the IF system. The wedging out pattern of sediment infill suggests syn-tectonic sedimentation along an active fault plane.

Seismic line CQ14_286 was collected in the flat region at the toe of the IF system where a slope terrace develops at the transition between the outer and inner accretionary wedges. The sedimentary basin in Figure 9e shows two depocenters separated by a rising feature which could be related to salt/mud diapirism triggered by tectonic processes. The zoom shows a clear wedging out pattern of the basin infill to the East suggesting syn-tectonic sedimentation. The transparent unit just below the seafloor is the HAT bed of Polonia et al. (2013) whose deposition was triggered by the AD 365 Crete earthquake and tsunami. The depressed geometry of the turbidite bed close to the normal fault suggests tectonic subsidence and active deformation reaching the seafloor.

Finally, Chirp seismic line CQ14_514 (Figure 9f) collected in the slope terrace at the toe of the IF system shows three fault scarps along which sediments are progressively downthrown and deformed. Along the fault planes roll-over anticlines are present suggesting a normal component

of movement. This evidence suggests that extensional processes are widespread in the Western Lobe which is progressively downthrown along a set of normal faults bounded on one side by the AEF and on the other side by the IF system.

3.2 – Morphotectonics of the accretionary wedge

Combined analysis of seismic reflection profiles (Figures 5-8) and morphobathymetric data in the Ionian Sea (Figure 2) suggests that major structural style variations occur between the EL and WL of the CA along the IF system. The EL has a tight arcuate shape that progressively gets narrower to the SE where it impinges against the Mediterranean Ridge (Figures 2 and 10) implying an incipient collision between the Calabrian and Hellenic Arcs. The accretionary wedge in this region shows a very rough morphology with km-scale ridges and troughs and steep topographic slopes. Conversely, the WL is a wide fan-shaped lobe, which reaches its maximum width and curvature at the contact with the abyssal plain. The outer accretionary wedge is characterised by very gentle slopes and a low-wavelength roughness as a response to sediment shortening on a shallow and very weak basal detachment (base of evaporites).

The AEF is marked to the North by a series of NNW-SSE oriented fault scarps, elongated ridges and submarine canyons with the same orientation of the fault trend (Figure 10). Towards the Alfeo seamount, in the deeper bathymetries, a major submarine canyon develops along the fault system, which disrupts the inner deformation front of the subduction complex (splay-3 in Figure 2). Tectonic deformation along the AEF leads to the formation of elongated Plio-Quaternary sedimentary basins, similarly to what observed for the IF system.

The IF system, i.e., the boundary between the two lobes, is a regional tectonic feature whose bathymetric signature is clearly expressed in the deeper basin by convergence of tectonic lineaments delimiting the two lobes. Here it is marked by a number of aligned, closely spaced

sedimentary basins, elongated in the NW-SE direction (Figures 9 and 10). The IF corresponds with the transition between a rather flat and depressed WL, and a rougher and topographically elevated EL (Figure 11). Dynamic topography in Calabria is reflected in high uplift rates of the coastal mountain belts, accompanied with a great sediment discharge to the continental margins. This increases the susceptibility to mass failures implying a strong interplay between active tectonics, seismic shaking and mass flows. Sediment remobilization and submarine landslides are triggered by the frequent occurrence of medium size earthquakes (Polonia et al., 2013 a) while more catastrophic events can produce dramatic sedimentary effects in the study area such as those related to the AD 365 Crete earthquake and associated tsunamis which triggered the deposition of a turbidite bed up to 25 m thick (Polonia et al., 2013b). The deposition of turbidite beds, which can be tens of meters thick, contribute to hamper the possibility to identify tectonic activity on the seafloor because sedimentation rate is higher than subsidence or uplift. Despite this limitation, high resolution seismic data (Figure 9) has shown the presence of active fault strands along the proposed IF; on the other hand, bathymetric profiles across the fault system (Figure 11) show a sharp transition with high bathymetric gradients which may be sustained by tectonic activity. In the region close to the Messina Straits, submarine canyons and topographic scarps sub-parallel to the IF system suggest they are tectonically controlled.

4 – Seismicity

In this section, we investigate the regional seismicity with special attention to faulting and style changes at the southwestern edge of the Ionian subducting slab.

4.1 - Data and methods

Figure 12 displays the epicenter maps (separated according to focal depth) of the earthquakes shallower than 300 km that occurred in Southern Italy between 1997 and 2012. Seismic data and recordings come from the Italian national network (<http://www.ingv.it>) and from the local networks operating in Calabria and Sicily (Neri *et al.* 2002; Barberi *et al.* 2004; Orecchio *et al.* 2011). Hypocenter locations were performed using the local 3D velocity model described in Orecchio *et al.* (2014) and the *Simul* linear location algorithm by Evans *et al.* (1994). The locations have been checked by means of the Bayloc earthquake location algorithm (Presti *et al.*, 2004, 2008) based on a non-linear probabilistic approach. For its structure and computational reasons, Bayloc is appropriate for testing linear locations of individual earthquakes or sets of earthquakes grouped in small volumes. The checks performed by Bayloc in several sectors over the whole region of Figure 12 allow us to conclude that the *Simul*'s maps reported in the same figure (which include the earthquakes of $M_d \geq 2.5$ characterized by at least 6 P and 8 P+S readings and $rms \leq 0.8$ sec) are accurate and suitable for the investigation. As often happens in this kind of practice, the location errors estimated by the non-linear method (Bayloc) are considerably more accurate (and larger) than formal errors furnished by the linearized algorithm (*Simul*) in the sectors where network geometry is not optimal. This is the case in the Ionian sector where much of the attention in the present study is focused (oblique box in Figure 12). Here, location errors on the order of 4 km (ERH) and 5 km (ERZ) are estimated by Bayloc for earthquakes deeper than 30 km, and slightly larger values of 5 km (ERH) and 6 km (ERZ) for shallower events.

A dataset of waveform inversion focal mechanisms relative to the period 1977-2012 was obtained for the area indicated by the box in Figure 12 (main study area) by integrating the solutions available from the official catalogues (<http://www.bo.ingv.it/RCMT/Italydataset.html>; <http://www.bo.ingv.it/RCMT/>; <http://cnt.rm.ingv.it/tdmt.html>), those estimated by Orecchio *et al.* (2014) with the CAP waveform inversion method (Zhao and Helmberger 1994; Zhu and Helmberger 1996), and seven additional solutions computed by CAP in the present study. The CAP solutions are characterized by fault parameter errors of less than 10° and great stability when

varying hypocenter locations inside the Bayloc uncertainty volumes. It is worth mentioning that CAP was successfully tested in the past for earthquakes over a wide range of magnitudes down to values as small as 2.6 (more details on the method and its stability features can be found in the papers by Tan *et al.* 2006, D'Amico *et al.* 2010, 2011). Our integrated dataset of selected high-quality focal mechanisms is reported in Figure 13 where the colored beach-balls identify the different types of faulting according to Zoback's standard classification (Zoback, 1992; see figure caption for details). We also show in figure 13b the polar plots of P- and T-axes relative to the whole set of focal mechanisms, the Alfeo-Etna Fault System zone and the Ionian Fault zone. In Figure 13c the focal mechanism solutions of earthquakes located around the Ionian Fault are projected along a NW-SE oriented vertical section also showing the P-wave velocity distribution from Neri *et al.* (2012).

4.2 Seismicity results

The seismicity shallower than 40 km reported in Figure 12a-b marks the main structural features of the Calabrian Arc region (Figure 1). In our main study area, in the western Ionian Sea, the seismic activity in the 20-40 km depth range is high relative to that in the 0-20 km range. The earthquakes occurring in the depth-range 40-70 km (Figure 12c) are mainly located offshore southern Calabria and a significant percentage of them lie close to the IF. The earthquakes deeper than 70 km (Figure 12d) are mainly located beneath the southern Tyrrhenian sea and in the inner subduction complex. Subcrustal earthquake activity (focal depth >40 km) predominantly occurs in the central part of the Calabrian Arc. This hypocenter distribution marks the location of the subducting Ionian lithosphere, in good agreement with the subducting slab signature furnished by Neri *et al.*'s (2009) Local Earthquake Tomography. The earthquake clustering observed near the IF zone, together with the other events in the 40-70 km depth range mainly located northeast of this same fault system (Figure 12c), suggests that the IF may correspond to the present-day lateral boundary of the Ionian lithospheric slab, as imaged by Neri *et al.*, (2009).

The high-quality focal mechanisms displayed in Figure 13a (for the events listed in Table 2) indicate mainly strike-slip faulting in the southwestern part of our main study area, e.g. near the AEF. Going to northeast, i.e. when approaching the IF, the same lateral-slip regime tends to coexist with normal faulting (Figure 13a), in agreement with the transtensional kinematics revealed by the combined analysis of morphobathymetric and seismic reflection data (see section 3.0). The transition from a nearly pure strike-slip regime near the AEF to a combination of strike-slip and normal faulting across the IF is highlighted by the distributions of P- and T-axes shown in Figure 13b. In particular, normal faulting earthquakes with focal depths of 36, 40 and 42 km (see earthquakes 13, 16 and 23 in Table 2 and Figure 13a) indicate a NE-SW extensional process in the IF zone acting on NW-trending fault planes nearly parallel to IF, e.g. perpendicular to trench. The focal depths of these events indicate that deformation occurs in the basement, below the accretionary wedge. In this connection see also Figure 13c, where Neri et al.'s (2012) reconstruction of upper/lower plate velocity structure highlights location of the quoted earthquakes in the downbending lithosphere. This reconstruction is supported by different data and information, such as (i) active seismic surveys (e.g., Nicolich et al., 2000; Cassinis et al., 2005), (ii) LET showing accumulation of highly-fractured fluid-enriched low-Vp high Vp/Vs materials closely over the de-hydrating retreating subduction slab (Barberi et al., 2004), (iii) velocity structure modeling based on joint analysis of data from active and passive seismology (Orecchio et al., 2011) and (iv) the lack of any eventual evidence of Ionian crust at depths deeper than the unique Moho discontinuity appearing in the vertical sections crossing the study area (Nicolich et al., 2000; Dezes and Ziegler, 2001; Barberi et al., 2004; Cassinis et al., 2005; Pontevivo and Panza, 2006; Neri et al., 2009 and 2012).

Because lithospheric deformation in a region of STEP activity is complex, the seismicity data do not cover a full seismic cycle, and a generally valid pattern for seismic activity associated with

STEPS is not (yet) available, we propose to compare seismicity in the Calabrian-Ionian area with regions which can be considered as type-localities for STEP action: the northern part of the Tonga subduction zone and the SE corner of the Caribbean plate, near Trinidad. For both regions a STEP-type tearing process has been invoked since the early stages of plate tectonics as an inevitable consequence of the plate boundary configuration (Isacks et al., 1969; Molnar and Sykes 1969). In particular, the northern Tonga zone is illustrative, because the extremely high convergence rate at the Tonga trench (up to 24 cm/yr near the northern end, Bevis et al. (1995)) is accompanied by intense STEP type activity at its northern end.

Interestingly, the complex deformation pattern in the northern Tonga zone encompasses normal faulting at depths of 52, 52 and 63 km, along WNW-ESE striking planes, i.e. approximately perpendicular to trench, hence parallel to STEP fault orientation (Millen and Hamburger, 1998; see their Figure 3). This was associated with the very first stages of tearing in the easternmost part of the study area. The focal depths indicate that the deformation occurred in the downbending part of the lithosphere, probably in the stage just prior to tearing, as proposed earlier by Forsyth (1975) for the northern end of the South Sandwich arc.

For the Trinidad region, the southern end of the Lesser Antilles subduction zone, Russo et al. (1993) and Marshall and Russo (2005) show very similar normal faulting in earthquakes with focal depths in the range of 50-56 km, in particular in the March 10, 1988 ($M_w=6.6$) event east of Trinidad and its aftershocks. Marshall and Russo (2005) interpreted this activity as part of the early stage of tearing of the lithosphere, in the vicinity of the tip of the tear. We note that this qualitative similarity in seismicity expression between the Tonga and Lesser Antilles subduction zones occurs in spite of an order of magnitude difference in convergence rate (~ 2 cm/yr for the Lesser Antilles subduction zone (DeMets et al., 2010) versus up to 24 cm/yr for Tonga (Bevis et al., 1995)).

The three dip-slip events 13, 16 and 23 (with focal depths 40, 42 and 36 km) in Fig 13a show similarities with the normal faulting events in the Northern Tonga and Trinidad regions, concerning a) the type of faulting and the orientation of nodal planes relative to strike of plate boundary, and b) the focal depth ranges, indicating deformation in the downbending lithosphere. When we compare the Trinidad region and Ionian Sea, which - in contrast with the Northern Tonga region- both have a well-developed accretionary wedge, we further note a similarity in epicentral location relative to the thrust front of the wedge. The very limited seismicity east-southeastward from these events is in agreement with the inference that the dip-slip events occurred near the tip of a propagating tear.

Thus, a comparison with well-known STEP regions leads us to conclude that distinct aspects of the regional seismicity in the Ionian realm are in support of STEP activity in the basement underlying the accretionary wedge, near the northwestern part of the Ionian Fault zone. The seismic activity near the AEF is discussed in section 6.2.

5 –Geodynamic model for Pliocene-Recent evolution

Despite the complexity of the onshore tectonic pattern, the activity of major fault systems agrees well with offshore data presented in this study, suggesting that the IF and AEF trending NNW-SSE to NW-SE may represent the Ionian counterparts of the dextral transtensive deformation zones as described onland. This interpretation fits with marine geophysical seismic data that suggest the presence of extensional processes between the Sicilian-Hyblean and the Ionian-Apulian blocks previously proposed by other authors based on different data (Nicolich et al., 2000; Goes et al., 2004; Rosenbaum and Lister, 2004; Chiarabba et al., 2008). This boundary separates the W-Calabria extensional belt from the N-Sicily contractional belt (Wortel and Spakman, 2000; Goes et al., 2004; Billi et al., 2006), and accommodates differential movements of

the Ionian accretionary wedge (Polonia et al., 2011, 2012). Considering that this plate boundary occurs above the approximate location where the SW edge of the slab is imaged, an interpretation in terms of a STEP fault is logical.

In this context, a key question is in which direction active STEPs propagate. In their numerical models, Govers and Wortel (2005) addressed this question, coming to the conclusion that the STEP will propagate in a direction that is approximately parallel to the STEP fault. However, their experiments were (deliberately) simple and did not consider the geological reality that passive margins and major faults may exist ahead of the STEP fault, with orientations that are significantly different from that of the STEP fault. Although they did not model it, Govers and Wortel (2005) did recognize that these features may have a steering effect which is why they suggested that the Malta Escarpement was the most recently activated part of the STEP fault near Sicily. Another relevant aspect is that the evolving slab geometry may lead to highly non-uniform slab pull forces nearby the active STEP. This may also have a steering effect on the propagation of the STEP. Both aspects were investigated using mechanical/numerical models (Nijholt and Govers, 2015). Here we present results of their work that are relevant for Calabria.

5.1 Model setup

We use the current geodynamic setting and geological record of the retreating Calabrian arc system in order to fashion a stylized mechanical model of the central Mediterranean setting. Regional deformation in the model is driven by the convergence of Africa (Nubia) and Europe in combination with the pull by the Ionian slab. A critical element is that the shape of the slab, and hence the slab pull, is made to agree with seismological constraints. Wortel and Spakman (2000) show that the Ionian slab can be traced down to the upper-lower mantle transition, with a 70° dip through the upper mantle. At its NE termination, slab detachment has occurred at the top, but the

slab is still attached to the Ionian slab in deeper parts of the upper mantle. At its SW termination, oblique rollback with respect to the passive margin has resulted in a narrowing trench, leading to a wider slab towards the bottom of the upper mantle. This slab geometry results in higher slab pull near the Sicilian and Apulian STEPs. In these stylized models, the convergent part of the plate contact is taken to be straight. We expect this simplification to affect the results only slightly.

The starting model geometry (Figure 14; Time 1) resembles the situation of the retreating Calabrian trench in the Early-Middle Pliocene, when slab detachment beneath central Italy was complete (Wortel and Spakman, 2000; van der Meulen et al., 2000). Here, the STEP had already propagated along the North African margin (Wortel et al., 2009) so that STEPs bound the plate contact on both ends. The corresponding STEP faults are modeled as low-friction vertical faults. The Calabrian trench is oriented in accordance with the iso-depth contour lines of the subducting slab as indicated in Figure 1 (Selvaggi and Chiarabba, 1995). At the trench, slab pull associated tractions are transmitted into the Ionian oceanic lithosphere and a trench suction force is acting on the Tyrrhenian basin. The active STEPs are located at the intersections of the trench and the STEP faults (indicated by solid red lines in Figure 14).

Nijholt and Govers (2015) model the passive margins as parallel bands at the ocean-continent boundary to employ a transition in material properties from an old oceanic (Ionian) lithosphere to the continental (African/Nubian) lithosphere. Here, continental lithosphere is taken to be mechanically weak (see Table 3 for mechanical properties). The Mesozoic Ionian basin is assumed to be mechanically strong. The mechanical strength of the young Tyrrhenian lithosphere is weak. Passive margins have intermediate strengths.

At the Apulian side of the trench the passive margin is taken to follow the trace of the Sangineto line, i.e., the geological border of the Calabrian domain with the Apennines. At the Sicilian side, the passive margin is oriented parallel to the trace of the Taormina line, i.e., the

geological border of the Calabrian domain in the NE and the Kabylean and Sicilian-Maghrebian belts in the SW (e.g., Finetti et al., 2005). East of the continental Nubian lithosphere, the Malta Escarpment is a Mesozoic weakness zone at the Nubian-Ionian lithosphere boundary. This lithospheric scale feature is incorporated in the model as a pre-existing strike-slip fault with low friction. Of the Alfeo-Etna fault, oriented about N150°E (grey dashed line; Polonia et al., 2012; Gallais et al., 2013) it is unclear whether it already existed before the Early-Middle Pliocene. We do not include it as a pre-existing feature in the models but, as we will see in the results below, this is inconsequential for the STEP propagation direction.

5.2 Results

In Figure 14, three important steps in the evolution of the retreating Calabrian arc are depicted. At Time 1 (Early-Middle Pliocene), the sense and rate of strike slip on both the northeastern and the south-southwestern STEP faults represent the response to shear stresses. Similarly, low-rate dextral shear is predicted along the Malta Escarpment. Strain localization and therefore STEP propagation tracks the passive margin in this time slice (and in following). Nijholt and Govers (2015) conclude that this response is typical for passive margins with small ($< 10^\circ$) variations in their orientation. An important element in the reconstruction at Time 1 is that the orientation of the passive margin at the southern end of the subduction zone changed orientation from roughly E-W north of Sicily, to the ESE along the Taormina line and parallel to the Sisifo fault (Billi et al. 2007). The model result shows that strain localizes ahead of the active STEP along this margin. This indicates that the change in orientation of the passive margin guides the STEP towards the ESE.

The geometry at (a later) Time 2 shows the situation when the active STEP has reached the passive margin bounding the Malta Escarpment. In keeping with the ideas of Goes et al. (2004),

the end of thrusting of the Sicilian nappes 1-0.8 Ma may correspond with Time 2. This turns out to be the decisive stage for the subsequent evolution. First, although the Malta Escarpment is represented by a low-friction fault in the model, the amount of predicted slip on the fault is close to zero. The angle between the Taormina line and the Malta Escarpment is too large to bridge for the STEP. This is shown by the pattern of strain localization that indicates that the STEP will propagate to the ESE.

Fracture zones and transform faults in the Ionian lithosphere probably define a NW-SE fabric (Frizon de Lamotte et al., 2011), which potentially were a significant element in directing the STEP. Such pre-existing faults that cut the Ionian lithosphere would be preferential locations for STEP propagations only if they (approximately) intersected the Taormina Line and the Malta Escarpment, and if their strike fell within the orange wedge. This thus excludes the Alfeo-Etna fault (grey dashed line) as the propagation direction for the STEP at this time. The mechanical model therefore favors the development of a lithosphere-breaking fault where the Ionian Fault is observed at present.

Panel Time 3 in Figure 14 represents the Present-day situation that follows from strain localization at and after Time 2. It shows the approximate location of the Ionian subduction contact (schematic, represented at the lithosphere scale), which is distinctly different from the location of the Calabrian trench. In this frame, the Tindari and Sisifo faults are taken to be active, in agreement with geological, seismological and geodetic observations (Billi et al., 2006, 2007). The Tindari fault does not directly connect to the Malta Escarpment (Billi et al., 2006). The same observations indicate that the Taormina line is presently inactive, which is why we do not allow slip along it. The STEP in the NE has propagated parallel to the Apulian escarpment. The STEP in the SW has propagated to the ESE since Time 2. The Alfeo-Etna fault falls outside the range of likely propagation directions, even if it existed already. The model results thus support the

interpretation of further lengthening (or reactivation) of the STEP fault zone in the lithosphere beneath the Ionian Fault in the innermost wedge.

Further analysis of the results at Time 3 shows that the model slip rate on this STEP fault varies between 5 mm/yr near Sicily, to 10 mm/yr near the active STEP. The dextral slip rate along the Malta Escarpment is <2 mm/yr. Tindari and Sisifo faults in the model show low rates of dextral slip. To the north of Sicily, compressional seismicity may indicate that subduction may be initiating here (Billi et al., 2007; Baes et al., 2011). In our stylized model, this shows as a stress concentration in the Tyrrhenian Sea.

The mechanical model is purposely kept simple to highlight the most important controls on STEP evolution, i.e., pre-existing geometry and strength contrast across the passive margin. The fact that the AEF is not activated by STEP propagation means that its tectonics require an explanation in broader, regional context (see section 6.2). The results of the numerical model experiments show to be relatively insensitive to smaller scale details (Nijholt and Govers, 2015). Our model representation of the STEP fault zone by a single, vertical discontinuity is schematic: it is expected to be wider in reality, as appears to be clear from the seismicity also.

Finally, we note that the numerical models represent the response of the basement to regional forces. The accretionary wedge is mechanically weak and therefore somewhat independent in its response to the lithospheric scale drivers. In the following section we therefore discuss the connection of the basement deformation and wedge tectonics.

6.0- Discussion

The IF and AEF systems represent the boundaries of a wide and complex deformation zone affecting the entire Western Lobe of the CA subduction complex in the Ionian Sea. This zone shows active tectonics along a set of southward diverging NW-SE trending fault strands (Figure 10)

with the IF and AEF systems being the main faults delimiting active transtensional tectonics. The fault strands located in between the IF and AEF and labelled F1, F2 and F3 in the structural map of Figure 10, offset splay faults at the contact between the inner and outer accretionary wedges (Polonia et al., 2011) and control the formation of sedimentary basins (Figures 7, 8, 9, 10). In the following sections we analyze the geodynamic significance of the IF and AEF together with their age and kinematics deduced through seismostratigraphic reconstructions. To clarify the ensuing discussion Figure 15 schematically shows the regional geodynamic context encompassing two principal components of lithospheric scale processes: 1) the Africa-Eurasia relative plate motion, and 2) the ESE retreat of the Calabrian slab.

6.1 - Geodynamic significance of the Ionian fault system.

The IF is a prominent feature all across the accretionary wedge from the eastern margin of Sicily to the deformation front in the ESE (Figure 10). Different processes can be proposed to explain the origin of the IF system.

- a) The IF system is related to the surface expression of lateral ramp accommodating the outward propagation of the Ionian accretionary prism. In this case, we should expect a strike-slip to reverse segmented system that shallows down at depth branching the main decollement of the thrust system. Our observations do not support this model as the Ionian fault system cross cut the main thrust system (Figure 8).
- b) The IF system is related to the rigid extrusion of the Calabrian block during backarc extension (Casero and Roure; 1994; Mantovani et al., 2002; Roure et al., 2012). In this case, we should expect a dextral strike-slip system that should end up towards SE on a system of horse tail-like NE-SW thrust system to accommodate extrusion. Our structural observation does not support this hypothesis (Figure 10).

- c) A variant of the model b) is that the IF system accommodates the indentation of the Pelagian block (Adam et al., 2000; Mantovani et al., 2002). In this case, we should expect that deformation should vanish moving northward. Our observations in fact show the contrary, i.e. deformation decreases southward.
- d) The last model is that the Ionian fault system is linked to the migration of the retreating hinge of the narrow Calabrian subduction zone (Figure 15). This process should likely deform the subducting plate, producing a STEP like feature (Doglioni et al., 2001; Gvirtzman and Nur, 1999; Govers and Wortel, 2005). For this model, we should expect deformation decreasing moving outward from the subducting slab and being active only during trench rollback. Our structural observations and numerical model test indeed support this model.

The available data and our model results indicates that the NW part of the IF, as a surface expression, corresponds with STEP activity in the underlying basement (Figure 15, yellow segment). Continuity with a corresponding crustal deformation pattern in NE Sicily (Palano et al., 2015) supports this interpretation. However, STEP activity as such does not explain the continuation of the IF toward the ESE, where it ends at the front of the Mediterranean Ridge (Figure 15). The migrating Calabria trench drives the entire accretionary wedge outward, but the two lobes of the wedge experience different boundary conditions: the eastern lobe collides with the Mediterranean Ridge, whereas the western lobe is free to spread into the abyssal plain of the Ionian Sea. Extensional faulting and basin formation, predominantly between the IF and the AEF, are an expression of this spreading. The ESE continuation of the IF represents the transition between the eastern and western lobes. We thus suspect that the NW part of the IF corresponds with basement activity associated with the STEP, and activity in the ESE part is an expression of collisional processes between the oppositely verging Calabrian and Hellenic subduction systems.

6.2 – Significance of the Alfeo-Etna system

The surface deformation and seismicity data, in combination with the modeling results, point to the IF as the present surface expression of the STEP activity at depth. The mechanical models indicate that the AEF is outside the region affected by STEP propagation at depth. As a consequence, dextral shear deformation along the AEF is not considered to be part of the Ionian slab related STEP activity and requires an alternative explanation. We propose that it results from regional scale shearing between central-western Sicily and the region to the east of this (Figure 15). In this part of the African plate, the differential motion underlying the shear deformation may result from west-east tectonic differences along the south Tyrrhenian margin (Billi et al., 2006; see also section 2.1). Seismicity and structural observations indicate that thrusting in its western and central parts (Billi et al., 2011) accommodates (part of) the convergence between Africa and the Tyrrhenian Sea (as part of Eurasia). Contrastingly, north-south thrusting is more limited or perhaps even absent in the eastern part of the south Tyrrhenian margin. This gives rise to the dextral shear corridor displayed in Figure 15 (see also Figure 10), with the AEF as a prominent feature in that corridor, W-SW of the STEP-related activity near the IF. This role of the AEF in the regional geodynamic setting accounts for a distinct difference in seismicity with respect to that near the IF (Figure 13a): whereas both regions exhibit dextral shear the lithosphere near the IF is involved in downbending (and tearing), causing extension, whereas downbending is absent towards the west-southwest, where differential horizontal motion dominates.

Recently Gutscher et al. (2015) published a detailed study of the Alfeo-Etna Fault (AEF) and surroundings. Using seismic and bathymetry data, in combination with available focal mechanisms, they documented dextral strike-slip motion along the northern part of the AEF and predominantly normal faulting, with possibly large dextral strike-slip motion, along the southern

part. The authors interpret the combined parts of the AEF as the surface expression of the STEP associated with the SW edge of the retreating Calabrian slab. In our study we study the AEF and the IF, jointly, in the context of the Africa-Eurasia convergence and deformation of the Calabrian Arc subduction complex. Shallow expressions of the AEF and IF are very similar (see Figure 7b), and both faults extend to the (E)SE well beyond the location of the lithospheric plate boundary (for the IF, the green part of the fault zone in Figure 15). Whereas for the IF the collision of the Calabrian Arc accretionary complex with that of the Hellenic Arc may account for the extension to the ESE of the IF beyond the active STEP (see section 6.1), it is not clear how this SE extension is accounted for in the Gutscher et al. (2015) interpretation of the AEF. In this context, it is important to keep in mind that the expected differential motion near the active STEP is vertical, and not strike-slip (Figure 15, inset). More importantly, the broader scope of our analysis, both in dimensions of the study area (including the lithospheric scale depth range) and in diversity of the data and research methodologies used, allows us to address the full lithospheric scale of the STEP related process, to compare the characteristics of the AEF and the IF and to identify the role of each of these two fault zones in the overall context of this complex plate boundary segment, as described above and illustrated in Figure 15.

6.3 - Age of fault inception and the Etna volcano

The analysis of MCS profiles suggests that four major tectonic phases shaped the continental margin since the Oligocene. A first Oligocene shortening was followed by extension in the late Miocene with sedimentary basins development (Figure 5). A subsequent post-Messinian basin inversion, lasting up to the middle-upper Pliocene, is marked by an angular unconformity in the Plio-Quaternary deposits (Figure 5). Finally, during Quaternary times, transtensive deformation on both sides of the WL produced a complex system of extensional faults re-activating old thrust

structures. This sequence of tectonic events correlates well with the onshore-offshore tectonic history reconstructed by Monaco et al. (1996) for the Messina Straits area, and the tectonic phases shaping the Squillace basin from Oligocene time (Capozzi et al., 2012).

Although MCS data suggest that the AEF and IF develop over structural boundaries inherited by the Mesozoic Tethyan basin and a complex Messinian deformation history, their recent tectonic activity fits well with the latest Quaternary extensional phase. In fact, fault inception along the AEF and IF produced the down throw of the WL and the formation of sedimentary basins (Figure 9) which are filled by up to 700-800 m of sediments (Figures 3c, 7, 8 and 9). This observation can be used to reconstruct the age of the fault, if sedimentation rate is known. In situ pelagic Holocene sedimentation rate in the working area is about $0.05-0.1 \text{ mka}^{-1}$ as deduced from the analysis of sediment cores collected in the region (Polonia et al., 2013a). However, sedimentation in the deep Ionian basin is mainly related to mass flow processes triggered by seismic shaking, which delivers more than 90% of the sedimentary sequence, with sedimentation rates 10-20 times higher relative to hemipelagic processes (Polonia et al., 2013b). This implies that 700 m of sediment thickness in basins along the IF and AEF might correspond to 350,000-700,000 yrs.

According to Hirn et al. (1997), the Mt. Etna volcanism developed in response to normal faulting, up-warping and spreading during the recent evolution of the Ionian subduction. Extensional processes and associated magmatism could be related to vertical upwelling of the asthenosphere at the SW lateral edge of the Ionian slab (Gvirtzman and Nur, 1999; Doglioni et al., 2001; Billi et al., 2010). Laboratory (Funciello et al., 2006) and numerical experiments (Piromallo et al., 2006) show that at the edges of a retreating slab we expect a toroidal component of asthenospheric flow. This may induce an upward flow and decompression melting which could well explain the formation of the Mt. Etna (Faccenna et al., 2011). After an earlier phase (500 ka and 330 ka) of discontinuous and scattered activity, the volcanism in Mt. Etna region between 220 and

121 ka ago was concentrated along the Ionian coast (Timpe phase of Branca et al., 2011). During this phase, the extensional tectonics of the Ionian margin of Sicily (Monaco et al., 1997, 2010; Azzaro et al., 2012) enhanced magma ascent, transforming the previous scattered fissural volcanism into an almost continuous volcanic activity that about 100 ka ago shifted westward to form the present large central edifice (Branca et al., 2011).

Even though a clear continuity between onshore and offshore structural boundaries was not verified so far due to the difficulty of collecting good-quality penetrative seismic images close to the coast, the SSE to SE trending fault systems observed in the Ionian Sea, mostly focused along the IF and AEF, may be interpreted as the prolongation of the Mt. Etna bounding faults described by Chiocci et al. (2011). This connection between large-scale offshore tectonic processes and the formation of the volcano seems to be also supported by the geometry and age of transtensive reactivation along the IF and the AEF, which might indicate a primary role played by a Pleistocene geodynamic re-organization in the western Ionian Sea in the Mt. Etna volcanism.

7- Conclusions

A multi-scale approach involving marine geophysics, seismology and regional geodynamic models suggest a recent (Middle Pleistocene) re-organization of the Africa/Eurasia plate boundary in the Ionian Sea.

Two sets of oppositely dipping fault systems are present on both sides of the western part of the accretionary wedge offshore Eastern Sicily. One system runs from the Alfeo seamount to the Etna volcano, the Alfeo-Etna fault system (AEF); the second dissects the submerged Calabrian Arc in the Ionian Sea and represents the boundary between the two lobes of the accretionary wedge (the Ionian fault, IF). Active deformation along transverse faults suggests a transtensional motion, associated with a complex deformation pattern involving strike-slip and normal faults,

sedimentary basins, ridges and morphological scarps. The IF and AEF systems mark a wide and complex deformation zone, which includes three more fault strands (F1, F2, F3) accommodating active transtensional tectonics.

Seismo-stratigraphic analysis reveals that transtensional faulting along the AEF and IF systems re-activates inherited structures of the lower African plate. This suggests that they could have been formed along oceanic fracture zones of the Tethyan domain, which acted as paleo-oceanographic boundaries during the Messinian salinity crisis, and accommodate plate boundary re-organization.

Despite the complexity of the onshore tectonic pattern, the activity of major fault systems agrees well with offshore data presented in this study. The IF and AEF may thus represent the Ionian counterparts of the dextral transtensive deformations described in NE Sicily and in the southern Tyrrhenian Sea.

Seismological data indicate that both fault systems are crustal boundaries accommodating transtensional deformation, in agreement with geodetic models suggesting plate divergence in the Western Ionian Sea.

Mechanical/numerical models designed to highlight the most important controls on STEP (Subduction-Transform Edge Propagator) faults evolution, suggest that fracture zones and transform faults in the Ionian lithosphere were significant elements in directing the STEP. However, pre-existing faults that cut the Ionian lithosphere (i.e. the AEF and IF) would be preferential locations for STEP propagations only if their strike fell within a range of likely propagation directions. This excludes the AEF as the propagation direction for the slab edge related STEP, even if it existed already, and favors the development of a lithosphere-breaking fault in the NW part of the zone where the IF is observed at present.

The model results thus support the propagation of the (Calabrian slab edge related) STEP in the lithosphere beneath the NW part of the IF in the wedge. However, STEP activity does not explain the continuation of the IF toward the ESE, where it ends at the front of the Mediterranean Ridge. The migrating Calabria trench drives the entire accretionary wedge outward, but the two lobes of the wedge experience different boundary conditions: the eastern lobe collides with the Mediterranean Ridge and produce basement-involved tectonics, whereas the western lobe is free to spread into the abyssal plain of the Ionian Sea. In this context, the NW part of the IF corresponds with basement activity associated with the STEP, and activity in the ESE part is an expression of collision between the Calabrian and Hellenic wedges.

The AEF is not activated by STEP propagation related to the SW edge of the Calabrian slab and its tectonics might be the result of regional scale lithospheric deformation connecting the thrust zone along the northern margin of Sicily with the Calabrian subduction, which gives rise to a dextral shear corridor including the Etna volcano and segments of the Malta escarpment. Both the IF and AEF are predominantly dextral, with varying degrees of transtension. Whereas downbending of the lithosphere is proposed as the specific cause of the tensional component for (the NW part of) the IF, the tensional component for AEF is considered to be part of the regional strain field associated with Africa-Eurasia relative motion.

Finally, our study shows that a multidisciplinary approach addressing the entire lithospheric scale of the region is needed to grasp the structure and process of STEPs and their surface expression. The deformation pattern is more complicated than the often given scissor-type, one distinct fault representation. Furthermore, the process is strongly dependent on regional aspects concerning large-scale plate motion and plate boundary setting. The Tyrrhenian-Sicily-Calabrian region illustrates this in a convincing way.

Acknowledgements

The CALAMARE scientific party, Captain Lubrano, Urania shipboard and SOPROMAR parties are greatly acknowledged for data acquisition during the Urania cruise. We greatly acknowledge the CIESM/*Ifremer Medimap group* (Loubrieu et al., 2008) for the multibeam grid of the study area. We thank P. Mussoni and M. Ligi for processing of seismic line CALA 02. Structural mapping has been performed with the SeisPrho software (Gasperini and Stanghellini, 2009) which is freely available at <http://software.bo.ismar.cnr.it/seisprho>. We are greatly indebted to A. L. Cazzola and A. Fattorini (ENI Spa) for having provided us with seismic line CA99-215. This work has been supported by MIUR-PRIN, 2010-11 (Project: Active and recent geodynamics of Calabrian Arc and accretionary complex in the Ionian Sea, coordinated by C. Monaco) and has benefited from funding provided by CNR for the R/V Urania cruise.

References

- Adam, J., Reuther, C. D., Grasso, M., & Torelli, L., 2000. Active fault kinematics and crustal stresses along the Ionian margin of southeastern Sicily. *Tectonophysics* 326(3), 217-239. doi:10.1016/S0040-1951(00)00141-4
- Aloisi, M., Bruno, V., Cannavò, F., Ferranti, L., Mattia, M., Monaco, C., Palano, M., 2012. Are the source models of the M 7.1 1908 Messina Straits earthquake reliable? Insights from a novel inversion and a sensitivity analysis of levelling data. *Geophys. J. Int.* 192,1025-1041.
- Amodio-Morelli, L., Bonardi, G., Colonna, V., Dietrich, D., Giunta, G., Ippolito, F., Liguori, V., Lorenzoni, S., Paglionico, A., Perrone, V., Piccarreta, G., Russo, M., Scandone, P., Zanetti-Lorenzoni, E., Zuppetta, A., 1976. L'Arco Calabro-Peloritano nell'orogene appenninico-maghrebide. *Memorie Società Geologica Italiana* 17, 1-60.
- Amoruso, A., Crescentini, L., Scarpa, R., 2002. Source parameters of the 1908 Messina Straits, Italy, earthquake from geodetic and seismic data. *J. Geophys. Res.* 107 (B4), 2080, doi:10.1029/2001JB000434.
- Argnani, A., Bonazzi, C., 2005. Malta Escarpment fault zone offshore eastern Sicily: Plio-Quaternary tectonic evolution based on new multichannel seismic data, *Tectonics*, 24, TC4009, doi:10.1029/2004TC001656.
- Azzaro R., Branca, S., Gwinner, K., Coltelli, M., 2012. The volcano-tectonic map of Etna volcano, 1:100.000 scale: an integrated approach based on a morphotectonic analysis from high-resolution DEM constrained by geologic, active faulting and seismotectonic data. *Ital. J. Geosci. (Boll.Soc.Geol.It.)* 131, 153-170. doi: 10.3301/IJG.2011.29
- Baes, M., Govers, R., Wortel, R., 2011. Subduction initiation along the inherited weakness zone at the edge of a slab: Insights from numerical models, *Geophysical Journal International* 184(3), 991–1008. doi:10.1111/j.1365-246X.2010.04896.
- Barberi G., Cosentino, M.T., Gervasi, A., Guerra, I., Neri, G., Orecchio, B., 2004. Crustal seismic tomography in the Calabrian Arc region, south Italy. *Physics of the Earth and Planetary Interiors* 147, 297–314. doi:10.1016/j.pepi.2004.04.005.

- Barreca, G., Bruno, V., Cocorullo, C., Cultrera, F., Ferranti, L., Guglielmino, F., Guzzetta, L., Mattia, M., Monaco, C., Pepe, F., 2014a. Geodetic and geological evidence of active tectonics in south-western Sicily (Italy). *J. of Geodynamics* 82, 138-149. doi:10.1016/j.jog.2014.03.004
- Barreca, G., Bruno, V., Cultrera, F., Mattia, M., Monaco, C., Scarfi, L., 2014b. New insights in the geodynamics of the Lipari–Vulcano area (Aeolian Archipelago, southern Italy) from geological, geodetic and seismological data. *J. of Geodynamics* 82, 150–167, doi:10.1016/j.jog.2014.07.003.
- Bevis, M., Taylor, F. W., Schutz, B. E., Recy, J., Isacks, B.L., Helua, S., Singhy, R., Kendrick, E., Stowell, J., Taylor, B., Calmant, S., 1995. Geodetic observations of very rapid convergence and backarc extension at the Tonga arc. *Nature* 374, 249-252, 1995. doi:10.1038/374249a0
- Bianca, M., Monaco, C., Tortorici, L., Cernobori, L., 1999. Quaternary normal faulting in southeastern Sicily (Italy): a seismic source for the 1693 large earthquake. *Geophys. J. Int.* 139, 370–394. doi: 10.1046/j.1365-246x.1999.00942.x
- Billi, A., Barberi, G., Faccenna, C., Neri, G., Pepe, F., Sulli, A., 2006. Tectonics and seismicity of the Tindari Fault System, southern Italy: Crustal deformation at the transition between ongoing contractional and extensional domains located above the edge of a subducting slab. *Tectonics* 25, TC2006. doi:10.1029/2004TC001763.
- Billi, A., Presti, D., Faccenna, C., Neri, N., Orecchio, B., 2007. Seismotectonics of the Nubia plate compressive margin in the south Tyrrhenian region, Italy: Clues for subduction inception, *J. Geophys. Res.* 112, B08302. doi:10.1029/2006JB004837.
- Billi, A., Presti, D., Orecchio, B., Faccenna, C., Neri, G., 2010. Incipient extension along the active convergent margin of Nubia in Sicily, Italy: Cefalù-Etna seismic zone. *Tectonics* 29, TC4026. doi:10.1029/2009TC002559.
- Billi, A., Faccenna, C., Bellier, O., Minelli, L., Neri, G., Piromallo, C., Presti, D., Scrocca, D., Serpelloni, E., 2011. Recent tectonic reorganization of the Nubia-Eurasia convergent boundary heading for the closure of the western Mediterranean. *Bull. Soc. Géol. de France* 182, 279-303.
- Bijwaard, H., Spakman, W., 2000. Non-linear global P-wave tomography by iterated linearized inversion. *Geophysical Journal International* 141, 71–82. doi:10.1046/j.1365-246X.2000.00053.x
- Bonardi, G., Cavazza, W., Peruarone, V., Rossi, S., 2001. Calabria-Peloritani terrane and northern Ionian Sea. In Vai, G. B., Martini, I. P., (Eds), *Anatomy of an Orogen: The Apennines and Adjacent Mediterranean Basins*, Kluwer Academic, Dordrecht, Netherlands, pp. 286–306.
- Branca S., Coltelli, M., Groppelli, G., Lentini, F., 2011. Geological map of Etna volcano, 1:50,000 scale, *Ital. J. Geosci.*, 130 (3), 265-291; doi: 10.3301/IJG.2011.15.
- Capozzi, R., Artoni, A., Torelli, L., Lorenzini, S., Oppo, D., Mussoni, P., Polonia, A., 2012. Neogene to Quaternary tectonics and mud diapirism in the Gulf of Squillace (Crotona-Spartivento Basin, Calabrian Arc, Italy). *Mar. Petrol. Geol.* 35, 219-234. doi:10.1016/j.marpetgeo.2012.01.007.
- Carminati, E., Wortel, M.J.R., Spakman, W., Sabadini, R., 1998. The role of slab detachment processes in the opening of the western–central Mediterranean basins: some geological and geophysical evidence. *Earth and Planetary Science Letters* 160, 651–665. doi:10.1016/S0012-821X(98)00118-6.
- Casero, P., Roure, F., 1994. Neogene deformations at the Sicilian–North African plate boundary. In Roure, F. (Ed.), *Peri-Tethyan platforms*, Editions Technip, Paris, pp. 27-50.
- Cassinis R., Scarascia S. and Lozej A.; 2005: Review of seismic Wide-Angle Reflection-Refraction (WARR) results in the Italian Region (1956-1987). In: Finetti I.R. (ed), *CROP PROJECT: Deep Seismic Exploration of the Central Mediterranean and Italy*, Elsevier, Amsterdam, pp. 31-55.
- Cernobori, L., Hirn, A., McBride, J. H., Nicolich, R., Petronio, L., Romanelli, M., and

- Streamers/Profiles Working Groups 1996. Crustal image of the Ionian basin and its Calabrian margins. *Tectonophysics* 264, 175–189. doi:10.1016/S0040-1951(96)00125-4.
- Chamot-Rooke, N., Rangin, C., Le Pichon, X., and DOTMED Working Group 2005. DOTMED–Deep Offshore Tectonics of the Mediterranean: A synthesis of deep marine data in eastern Mediterranean [CD-ROM]. *Mem. Soc. Geol. Fr.* 177, 64 pp.
- Chiarabba, C., De Gori, P., Speranza, F., 2008. The southern Tyrrhenian subduction zone. Deep geometry, magmatism and Plio-Pleistocene evolution. *Earth Planet. Sci. Lett.* 268, 408–423. doi:10.1016/j.epsl.2008.01.036.
- Chiocci, L.F., Coltelli, M., Bosman, A., Cavallaro, D., 2011. Continental margin large-scale instability controlling the flank sliding of Etna volcano. *Earth and Planetary Science Letters* 305 (1–2), 57–64. doi:10.1016/j.epsl.2011.02.040.
- Cuppari, A., Colantoni, P., Gabbianelli, G., Morelli, D., Alparone, R., 1999. Assetto ed evoluzione 596 morfo-strutturale dell'area marina compresa tra il margine della Sicilia settentrionale e le Isole 597 Eolie (Golfo di Patti), *Atti Ass. It. Ocean. Limnol.*, XIII, 137–149. http://www.aiol.info/vol/13.1_AIOL.pdf
- D'Agostino, N., Selvaggi, G., 2004. Crustal motion along the Eurasia-Nubia plate boundary in the Calabrian Arc and Sicily and active extension in the Messina Straits from GPS measurements. *J. Geophys. Res.* 109, B11402. doi:10.1029/2004JB002998.
- D'Agostino, N., Avallone, A., Cheloni, D., D'Anastasio, E., Mantenuto, S., Selvaggi, G., 2008. Active tectonics of the Adriatic region from GPS and earthquake slip vectors. *J. Geophys. Res.* 113, B12413. doi:10.1029/2008JB005860.
- D'Amico S., Orecchio, B., Presti, D., Zhu, L., Herrmann, R.B., Neri, G., 2010. Broadband waveform inversion of moderate earthquakes in the Messina Straits, southern Italy. *Physics of the Earth and Planetary Interiors* 179, 97–106. doi:10.1016/j.pepi.2010.01.012.
- D'Amico S., Orecchio, B., Presti, D., Gervasi, A., Zhu, L., Guerra, I., Neri, G., Herrmann, R.B., 2011. Testing the stability of moment tensor solutions for small earthquakes in the Calabro-Peloritan Arc region (southern Italy). *Bollettino di Geofisica Teorica ed Applicata* 52 (2), 283–298.
- De Astis G., Peccerillo, A., Kempton, P. D., La Volpe, L., Wu, T. W., 2000. Transition from calc-alkaline to potassium-rich magmatism in subduction environments: geochemical and Sr, Nd, Pb isotopic constraints from the island of Vulcano (Aeolian arc). *Contributions to Mineralogy and Petrology* 139 (6), 684–703.
- De Astis, G., Ventura, G., Vilardo, G., 2003. Geodynamic significance of the Aeolian volcanism (Southern Tyrrhenian Sea, Italy) in light of structural, seismological, and geochemical data. *Tectonics* 22, 1040. doi:10.1029/2003TC001506, 4.
- De Guidi G., Lanzafame, G., Palano, M., Puglisi, G., Scaltrito, A., Scarfi, L., 2013. Multidisciplinary study of the Tindari Fault (Sicily, Italy) separating ongoing contractional and extensional compartments along the active Africa–Eurasia convergent boundary. *Tectonophysics* 588, 1–17. <http://dx.doi.org/10.1016/j.tecto.2012.11.021>.
- De Guidi, G., Barberi, G., Barreca, G., Bruno, V., Cultrera, F., Grassi, S., Imposa, S., Mattia, M., Monaco, C., Scarfi, L., Scudero, S., 2015. Geological, seismological and geodetic evidence of active thrusting and folding south of Mt. Etna (eastern Sicily): reevaluation of “seismic efficiency” of the Sicilian Basal Thrust. *J. Geodynamics* 90, 32–41. doi:10.1016/j.jog.2015.06.001
- Del Ben, A., Barnaba, C., Taboga, A., 2008. Strike-slip systems as the main tectonic features in the Plio-Quaternary kinematics of the Calabrian Arc. *Mar. Geophys. Res.* 29, 1–12. doi:10.1007/s11001-007-9041-6.

- DeMets., C., Gordon, R.G., Argus, D.F., 2010. Geologically current plate motions. *Geophys. J. Int.* 181, 1-80.
- Devoti, R., Esposito, A., Pietrantonio, G., Pisani, A.R., Riguzzi, F., 2011. Evidence of large scale deformation patterns from GPS data in the Italian subduction boundary. *Earth Planet. Sci. Lett.* 311, 230–241. doi:10.1016/j.epsl.2011.09.034.
- Dèzes P. and Ziegler P.A.; 2001: European Map of the Mohorovicic discontinuity. In: 2nd EUCOR-URGENT Workshop (Upper Rhine Graben Evolution and Neotectonics), Mt. St. Odile, France.
- Dogliani, C., Merlini, S., Cantarella, G., 1999. Foredeep geometries at the front of the Apennines in the Ionian Sea (central Mediterranean). *Earth Planet. Sci. Lett.* 168, 243–254. doi:10.1016/S0012-821X(99)00059-X.
- Dogliani, C., Innocenti, F., Mariotti, G., 2001. Why Mt Etna? *Terra Nova* 13(1), 25–31. doi:10.1046/j.1365-3121.2001.00301.x.
- Dogliani C., Ligi, M., Scrocca, D., Bigi, S., Bortoluzzi, G., Carminati, E., Cuffaro, M., D'Orlando, F., Forleo, V., Muccini, F., Riguzzi, F., 2012. The tectonic puzzle of the Messina area (Southern Italy): Insights from new seismic reflection data. *Sci. Rep.* 2, 970. doi:10.1038/srep00970.
- Evans J.R., Eberhart-Phillips, D., Thurber, C.H., 1994. User's manual for simulps12 for imaging Vp and Vp/Vs: a derivative of the "Thurber" tomographic inversion simul3 for local earthquakes and explosions. Open File Report, USGS, Menlo Park, pp. 94-431.
- Faccenna, C., Becker, T. W., Lucente, F. P., Jolivet, L., Rossetti, F., 2001a. History of subduction and back-arc extension in the central Mediterranean. *Geophys. J. Int.* 145, 809–820. doi:10.1046/j.0956-540x.2001.01435.x.
- Faccenna C., Funicello, F., Giardini, D., Lucente, P., 2001b. Episodic back-arc extension during restricted mantle convection in the Central Mediterranean. *Earth and Planetary Science Letters* 187 (1–2), 105–116. DOI: 10.1016/S0012-821X(01)00280-1.
- Faccenna, C., Piromallo, C., Crespo-Blanc, A., Jolivet, L., Rossetti, F., 2004. Lateral slab deformation and the origin of the western Mediterranean arcs. *Tectonics* 23, TC1012. doi:10.1029/2002TC001488.
- Faccenna C., Funicello, F., Civetta, L., D'Antonio, M., Moroni, M., Piromallo, C., 2007. Slab disruption, mantle circulation, and the opening of the Tyrrhenian basins. In Beccaluva, L., Bianchini, G., Wilson, M., (Eds.), *Cenozoic Volcanism in the Mediterranean Area*. Geological Society of America Special Paper, 41, 153-169. doi: 10.1130/2007.2418(08).
- Faccenna, C., Molin, P., Orecchio, B., Olivetti, V., Bellier, O., Funicello, F., Minelli, L., Piromallo, C., Billi, A., 2011. Topography of the Calabria subduction zone (southern Italy): Clues for the origin of Mt. Etna. *Tectonics* 30, TC1003. doi:10.1029/2010TC002694.
- Favalli M., Karátson, D., Mazzuoli, R., Pareschi, M.T., Ventura, G., 2005. Volcanic geomorphology and tectonics of the Aeolian archipelago (Southern Italy) based on integrated DEM data. *Bulletin of Volcanology* 68(2), 157-170. DOI 10.1007/s00445-005-0429-3.
- Ferranti L., Oldow, J.S., D'Argenio, B., Catalano, R., Lewis, D., Marsella, E., Avellone, G., Maschio, L., Pappone, G., Pepe, F., Sulli, A., 2008. Active deformation in Southern Italy, Sicily and southern Sardinia from GPS velocities of the Peri-Tyrrhenian Geodetic Array (PTGA). *Boll. Soc. Geol. It. (Ital. J. Geosci.)* 127(2), 299–316.
- Finetti, I.R., Lentini, F., Carbone, S., Del Ben, A., Di Stefano, A., Forlin, E., Guarnieri, P., Pipan, M., Prizzon, A., 2005. Geological outline of Sicily and lithospheric tectono-dynamics of its Tyrrhenian margin from new CROP seismic data. In: Finetti, I.R. (Ed.), *CROP Project: Deep seismic exploration of the Central Mediterranean and Italy*, Elsevier, Amsterdam, pp. 319–375.
- Forsyth, D. W., 1975. Fault plane solutions and tectonics of the South Atlantic and Scotia Sea. *J. Geophys. Res.* 80, 1429-1443.

- Frizon de Lamotte, D., Raulin, C., Mouchot, N., Wrobel-Daveau, J.-C., Blanpied, C., Ringenbach, J.-C., 2011. The southernmost margin of the Tethys realm during the Mesozoic and Cenozoic: initial geometry and timing of the inversion processes. *Tectonics* 30, 1–22 TC3002. <http://dx.doi.org/10.1029/2010TC002691>.
- Funiciello, F., Moroni, M., Piromallo, C., Faccenna, C., Cenedese, A., Bui, H. A., 2006. Mapping mantle flow during retreating subduction: Laboratory models analyzed by feature tracking. *J. Geophys. Res.* 111, B03402. doi:10.1029/2005JB003792.
- Gallais, F., Graindorge, D., Gutscher, M.A., Klaeschen, D., 2013. Propagation of a lithospheric tear fault (STEP) through the western boundary of the Calabrian accretionary wedge offshore eastern Sicily (Southern Italy). *Tectonophysics* 602, 141–152. doi:10.1016/j.tecto.2012.12.026
- Gallais F., Gutscher, M. A., Klaeschen, D., Graindorge, D., 2012. Two-stage growth of the Calabrian accretionary wedge in the Ionian Sea (Central Mediterranean): Constraints from depth-migrated multichannel seismic data. *Marine Geology* 326–328, 28–45. <http://dx.doi.org/10.1016/j.margeo.2012.08.006>
- Gasperini, L., Stanghellini, G., 2009. SeisPrho: An interactive computer program for processing and interpretation of high-resolution seismic reflection profiles. *Comput. Geosci.* 35, 1497–1507, doi:10.1016/j.cageo.2008.04.014.
- Giacomuzzi, G., Civalleri, M., De Gori, P., Chiarabba, C., 2012. A 3D Vs model of the upper mantle beneath Italy: Insight On the geodynamics of the central Mediterranean, *Earth Planet. Sci. Lett.* 335–336, 105–120. Doi:10.1016/j.epsl.2012.05.004.
- Giunta, G., Luzio, D., Agosta, F., Calò, M., Di Trapani, F., Giorgianni, A., Oliveri, E., Orioli, S., Perniciaro, M., Vitale, M., Chiodi, M., Adelfio, G., 2009. An integrated approach to investigate the seismotectonics of northern Sicily and southern Tyrrhenian. *Tectonophysics*, 476, 13–21. doi:10.1016/j.tecto.2008.09.031
- Goes, S., Giardini, D., Jenny, S., Hollenstein, C., Kahle, H.-G., Geiger, A., 2004. A recent tectonic reorganization in the south-central Mediterranean. *Earth Planet. Sci. Lett.* 226, 335–345. doi:10.1016/j.epsl.2004.07.038.
- Govers, R., Wortel, M. J. R., 2005. Lithosphere tearing at STEP faults: Response to edges of subduction zones. *Earth Planet. Sci. Lett.*, 236, 505–523. doi:10.1016/j.epsl.2005.03.022.
- Grasso, M., 2001. The Apenninic—Maghrebien orogen in southern Italy, Sicily and adjacent areas. In Vai, G. B., Martini, I. P., (Eds.), *Anatomy of an Orogen: The Apennines and Adjacent Mediterranean Basins*, Kluwer Academic, Dordrecht, Netherlands, pp. 255–286.
- Gueguen, E., Doglioni, C., Fernandez, M., 1998. On the post-25 Ma geodynamic evolution of the western Mediterranean. *Tectonophysics* 298, 259–269. doi:10.1016/S0040-1951(98)00189-9.
- Gutscher, M.-A., Dominguez, S., Mercier de Lepinay, B., Pinheiro, L., Gallais, F., Babonneau, N., Cattaneo, A., Le Faou, Y., Barreca, G., Micallet, A., Rovere, M., 2015. Tectonic expression of an active slab tear from high-resolution seismic and bathymetric data offshore Sicily (Ionian Sea), *Tectonics* 34, doi:10.1002/2015TC003898.
- Gvirtzman, Z., Nur, A., 1999. The formation of Mount Etna as the consequence of slab rollback. *Nature* 401, 782–785. doi:10.1038/44555.
- Hirn, A., Nicolich, R., Gallart, J., Laigle, M., Cernobori, L., and Group Etna Seis, 1997. Roots of Etna volcano in faults of great earthquakes. *Earth Plan. Sc. Lett.* 148, 171–191.
- Isacks, B., Sykes, L., Oliver, J., 1969. Focal mechanisms of deep and shallow earthquakes in the Tonga-Kermadec region and the tectonics of island arcs. *Geol. Soc. Amer. Bull.* 80, 1443 – 1470.
- Jacques, E., Monaco, C., Tapponnier, P., Tortorici, L., Winter, T., 2001. Faulting and earthquake triggering during the 1783 Calabria seismic sequence, *Geophys. J. Int.* 147, 499–516. doi:10.1046/j.0956-540x.2001.01518.x.

- Jolivet, L., Faccenna, C., 2000. Mediterranean extension and the Africa-Eurasia collision. *Tectonics* 19, 1095–1106. doi:10.1029/2000TC900018.
- Lavecchia, G., Ferrarini, F., De Nardis, R., Visini, F., Barbano, M.S., 2007. Active thrusting as a possible seismogenic source in Sicily (Southern Italy): some insights from integrated structural-kinematic and seismological data. *Tectonophysics* 445, 145–167. doi:10.1016/j.tecto.2007.07.007.
- Lentini, F., Catalano, S., Carbone, S. 2000. Carta Geologica della Provincia di Messina, Scala 1:50.000, S.EL.CA, Firenze.
- Loubrieu B., Mascle, J., et al. 2008. Morpho-bathymetry of the Mediterranean Sea, CIESM/Ifremer Medimap Group, CIESM edition.
- Malinverno, A., Ryan, W. B. F., 1986. Extension in the Tyrrhenian Sea and shortening in the Apennines as result of arc migration driven by sinking of the lithosphere. *Tectonics* 5, 227–245. doi:10.1029/TC005i002p00227.
- Mantovani, E., Albarello, D., Babbucci, D., Tamburelli, C., Viti, M., 2002. Trench-arc-backarc systems in the Mediterranean area: examples of extrusion tectonics. *Journal of the Virtual Explorer*, 8, 131-147.
- Marshall, J. L., Russo, R. M., 2005. Relocated aftershocks of the March 10, 1988 Trinidad earthquake: Normal faulting, slab detachment and extension at upper mantle depths. *Tectonophysics* 398(3–4), 101–114. doi:10.1016/j.tecto.2004.11.010.
- Mastrolembo Ventura, B., Serpelloni, E., Argnani, A., Bonforte, A., Bürgmann, R., Anzidei, M., Baldi, P., Puglisi, G., 2014. Fast geodetic strain-rates in eastern Sicily (southern Italy): New insights into block tectonics and seismic potential in the area of the great 1693 earthquake. *Earth and Planetary Science Letters* 404, 77–88. <http://dx.doi.org/10.1016/j.epsl.2014.07.025>
- Mattia, M., Palano, M., Bruno, V., Cannavò, F., Bonaccorso, A., Gresta, S., 2008. Tectonic features of the Lipari–Vulcano complex (Aeolian archipelago, Italy) from 10 years (1996–2006) of GPS data. *Terra Nova* 20, 370–377. doi: 10.1111/j.1365-3121.2008.00830.x
- Mattia, M., Palano, M., Bruno, V., Cannavò, F., 2009. Crustal motion along the Calabro-Peloritan Arc as imaged by twelve years of measurements on a dense GPS network. *Tectonophysics* 476, 528-537. doi:10.1016/j.tecto.2009.06.006.
- Millen, D. W., Hamburger, M. W., 1998. Seismological evidence for tearing of the Pacific plate at the northern termination of the Tonga subduction zone. *Geology*, 26(7), 659 – 662. doi: 10.1130/0091-7613(1998)026<0659:SEFTOT>2.3.CO;2
- Minelli, L., Faccenna, C., 2010. Evolution of the Calabrian accretionary wedge (central Mediterranean). *Tectonics* 29, TC4004. doi:10.1029/2009TC002562.
- Molnar, P., Sykes, L. R., 1969., *Tectonics of the Caribbean and Middle America regions from focal mechanisms and seismicity*. *Geol. Soc. Am. Bull.* 80, 1639-1684.
- Monaco, C., Tapponnier, P., Tortorici, L., Gillot, P.Y., 1997. Late Quaternary slip rates on the Acireale-Piedimonte normal faults and tectonic origin of Mt. Etna (Sicily). *Earth Planet. Sci. Lett.* 147, 125-139. doi:10.1016/S0012-821X(97)00005-8.
- Monaco, C., De Guidi, G., Ferlito, C., 2010. The morphotectonic map of Mt. Etna. *Boll. Soc. Geol. It.* 129 (3), 408-428.
- Monaco, C., Tortorici, L., 2000. Active faulting in the Calabrian arc and eastern Sicily. *Journal of Geodynamics* 29, 407–424. doi:10.1016/S0264-3707(99)00052-6.
- Monaco, C., Tortorici, L., Nicolich, R., Cernobori, L., Costa, M., 1996. From collisional to rifted basins: An example from the southern calabrian arc (Italy). *Tectonophysics* 266, 233-249. doi:10.1016/S0040-1951(96)00192-8.

- Morelli, A., Barrier, E., 2004. Geodynamic Maps of the Mediterranean – sheet 2: Seismicity and Tectonics. Commission for the Geological Map of the World (CGMW) & Unesco, 1:13.000.000 scale.
- Neri, G., Barberi, G., Oliva, G., Orecchio, B., 2005. Spatial variations of seismogenic stress orientations in Sicily, south Italy. *Physics of the Earth and Planetary Interiors* 148, 175–191. doi:10.1016/j.pepi.2004.08.009.
- Neri, G., Barberi, G., Orecchio, B., Aloisi, M., 2002. Seismotomography of the crust in the transition zone between the southern Tyrrhenian and Sicilian tectonic domains. *Geophysical Research Letters* 29 (23), 2135. DOI: 10.1029/2002GL015562.
- Neri, G., Orecchio, B., Totaro, C., Falcone, G., Presti, D., 2009. Subduction beneath southern Italy close the ending: Results from seismic tomography. *Seismol. Res. Lett.* 80, 63–70. doi:10.1785/gssrl.80.1.63.
- Neri, G., Marotta, A. M., Orecchio, B., Presti, D., Totaro, C., Barzaghi, R., Borghi, A., 2012. How lithospheric subduction changes along the Calabrian Arc in southern Italy: geophysical evidences. *International Journal of Earth Sciences* 101 (7), 1949–1969. DOI 10.1007/s00531-012-0762-7
- Nicolich, R., Laigle, M., Hirn, A., Cernobori, L., Gallart, J., 2000. Crustal structure of the ionian margin of Sicily: Etna volcano in the frame of regional evolution. *Tectonophysics* 329, 121–139. doi:10.1016/S0040-1951(00)00192-X.
- Nicolosi, I., Speranza, F., Chiappini, M., 2006. Ultrafast oceanic spreading of the Marsili Basin, southern Tyrrhenian Sea: Evidence from magnetic anomaly analysis. *Geology* 34(9), 717–720. doi: 10.1130/G22555.1.
- Nijholt N., Govers R., 2015. The role of passive margins on the evolution of Subduction-Transform Edge Propagators (STEPS). *J. Geophys. Res., Solid Earth*, 10.1002/2015JB012202.
- Oldow, J.S., Ferranti, L., Lewis, D.S., Campbell, J.K., D'Argenio, B., Catalano, R., Pappone, G., Carmignani, L., Conti, P., Aiken, C.L.V., 2002. Active fragmentation of Adria, the north African promontory, central Mediterranean orogeny. *Geology* 30, 779–782. doi: 10.1130/0091-7613(2002)030<0779:AFOATN>2.0.CO;2.
- Orecchio, B., Presti, D., Totaro, C., Guerra, I., Neri, G., 2011. Imaging the velocity structure of the calabrian arc region (southern Italy) through the integration of different seismological data. *Bollettino di Geofisica Teorica ed Applicata* 52 (4), 625–638.
- Orecchio, B., Presti, D., Totaro, C., Neri, G., 2014. What earthquakes say concerning residual subduction and STEP dynamics in the Calabrian Arc region, south Italy. *Geophys. J. Int.* 199 (3),1929–1942. doi:10.1093/gji/ggu373
- Özbakır, A. D., Şengör, A. M. C., Wortel, M. J. R., Govers, R., 2013. The Pliny–Strabo trench region: A large shear zone resulting from slab tearing. *Earth and Planetary Science Letters* 375, 188–195. doi:10.1016/j.epsl.2013.05.025
- Palano, M., Ferranti, L., Monaco, C., Mattia, M., Aloisi, M., Bruno, V., Cannavò, F., Siligato, G., 2012. GPS velocity and strain fields in Sicily and southern Calabria, Italy: Updated geodetic constraints on tectonic block interaction in the central Mediterranean. *J. Geophys. Res.* 117, B07401. doi: 10.1029/2012JB009254.
- Palano, M., Schiavone, D., Loddo, M., Neri, M., Presti, D., Quarto, R., Totaro, C., Neri, G., 2015. Active upper crust deformation pattern along the southern edge of the Tyrrhenian subduction zone (NE Sicily): Insights from a multidisciplinary approach. *Tectonophysics* 657, 2015–218.
- Panieri, G., Polonia, A., Lucchi, R.G., Zironi, S., Capotondi, L., Negri, A., Torelli, L., 2013. Mud volcanoes along the inner deformation front of the Calabrian Arc accretionary wedge (Ionian Sea). *Marine Geology*, 336, 84–98. <http://dx.doi.org/10.1016/j.margeo.2012.11.003>.

- Patacca, E., Sartori, R., Scandone, P., 1990. Tyrrhenian basin and Apenninic arcs: Kinematic relation since Late Tortonian times. *Mem. Soc. Geol. Ital.* 45, 425–451.
- Pepe F., Sulli A., Bertotti G., Catalano R., 2005. Structural highs formation and their relationship to sedimentary basins in the north Sicily continental margin (southern Tyrrhenian Sea): Implication for the Drepano Thrust Front. *Tectonophysics*, 409, 1 – 18.
- Piromallo, C., Becker, T. W., Funicello, F., Faccenna, C., 2006. Three-dimensional instantaneous mantle flow induced by subduction. *Geophys. Res. Lett.* 33, L08304. doi:10.1029/2005GL025390.
- Polonia, A., Torelli, L., Mussoni, P., Gasperini, L., Artoni, A., Klaeschen, D., 2011. The Calabrian Arc subduction complex in the Ionian Sea: Regional architecture, active deformation, and seismic hazard. *Tectonics* 30, TC5018. doi:10.1029/2010TC002821.
- Polonia, A., Torelli, L., Gasperini, L., Mussoni, P., 2012. Active faults and historical earthquakes in the Messina Straits area (Ionian Sea). *Nat. Hazards Earth Syst. Sci.* 12, 2311-2328. doi:10.5194/nhess-12-2311-2012.
- Polonia, A., Panieri, G., Gasperini, L., Gasparotto, G., Bellucci, L.G., Torelli, L., 2013a. Turbidite paleoseismology in the Calabrian Arc subduction complex (Ionian Sea). *Geochemistry Geophysics Geosystem* 14, 112 – 140. Doi:10.1029/2012GC004402.
- Polonia, A., Bonatti, E., Camerlenghi, A., Lucchi, R. G., Panieri, G., Gasperini, L., 2013b. Mediterranean megaturbidite triggered by the AD 365 Crete earthquake and tsunami. *Scientific Reports*, 3, 1285. DOI: 10.1038/srep01285.
- Pontevivo A. and Panza G.F.; 2006: The lithosphere-asthenosphere system in the Calabrian Arc and surrounding seas - southern Italy. *Pure Appl. Geophys.*, 163, 1617-1659, DOI 10.1007/s00024-006-0093-3.
- Presti, D., Orecchio, B., Falcone, G., Neri, G., 2008. Linear versus non-linear earthquake location and seismogenic fault detection in the southern Tyrrhenian sea, Italy. *Geophysical Journal International* 172 (2), 607-618. doi: 10.1111/j.1365-246X.2007.03642.x.
- Presti, D., Troise, C., De Natale, G., 2004. Probabilistic location of seismic sequences in heterogeneous media. *Bulletin of Seismological Society of America* 94(6), 2239-2253.
- Rehault, J.P., Boillot, G., Mauffret, A., 1984. The western Mediterranean Basin geological Evolution. *Marine Geology* 55, 447–477.
- Reitz, M. A., Seeber, L., 2012. Arc-parallel strain in a short rollback-subduction system: The structural evolution of the Croton basin (northeastern Calabria, southern Italy). *Tectonics* 31, TC4017. doi:10.1029/2011TC003031.
- Rosenbaum, G., Lister, G. S., 2004. Neogene and Quaternary rollback evolution of the Tyrrhenian Sea, the Apennines, and the Sicilian Maghrebides. *Tectonics* 23, TC1013. doi:10.1029/2003TC001518.
- Rosenbaum, G., Lister, G. S., Duboz, C., 2002. Reconstruction of the tectonic evolution of the western Mediterranean since the Oligocene. In Rosenbaum, G., Lister, G. S., (Eds.), *Reconstruction of the evolution of the Alpine-Himalayan Orogen*, *Journal of the Virtual Explorer*, 8, pp. 107 - 130.
- Rosenbaum, G., Gasparon, M., Lucente, F. P., Peccerillo, A., Miller, M. S., 2008. Kinematics of slab tear faults during subduction segmentation and implications for Italian magmatism. *Tectonics* 27, TC2008. doi:10.1029/2007TC002143.
- Roure, F., Casero, P., Addoum, B., 2012. Alpine inversion of the North African margin and delamination of its continental lithosphere. *Tectonics* 31(3), TC3006), <http://dx.doi.org/10.1029/2011TC002989>

- Russo, R. M., Speed, R. C., Okal, E. A., Shepherd, J. B., Rowley, K. C., 1993. Seismicity and tectonics of the southeastern Caribbean. *J. Geophys. Res.* 98(B8), 14,299–14,319. doi:10.1029/93JB00507.
- Scarfi, L., Langer, H., Scaltrito, A., 2005. Relocation of microearthquake swarms in the Peloritani mountains – implications on the interpretation of seismotectonic patterns in NE Sicily, Italy. *Geophys. J. Int.* 163, 225–237. doi: 10.1111/j.1365-246X.2005.02720.x.
- Scarfi, L., Langer, H., Scaltrito, A., 2009. Seismicity, seismotectonics and crustal velocity structure of the Messina Strait (Italy). *Phys. Earth Planet. Int.* 177, 65–78. doi: 10.1016/j.pepi.2009.07.010.
- Scarfi L., Messina, A., Cassisi, C., 2013. Sicily and southern Calabria focal mechanism database: a valuable tool for local and regional stress-field determination. *Annals of Geophysics* 56(1), D0109, 1–17. doi:10.4401/ag-6109
- Selvaggi, G., Chiarabba, C., 1995. Seismicity and P-wave velocity image of the southern Tyrrhenian subduction zone. *Geophys. J. Int.* 121, 818–826. doi:10.1111/j.1365-246X.1995.tb06441.x.
- Serpelloni, E., Anzidei, M., Baldi, P., Casula, G., Galvani, A., 2005. Crustal velocity and strain-rate fields in Italy and surrounding regions: new results from the analysis of permanent and non-permanent GPS networks. *Geophys. J. Int.* 161(3), 861–880. doi:10.1111/j.1365-246X.2005.02618.x
- Tan Y., Zhu, L., Helmberger, D., Saikia, C., 2006. Locating and modeling regional earthquakes with two stations. *Journal of Geophysical Research* 111, B01306, B1,2156–2202. <http://dx.doi.org/10.1029/2005JB003775>
- Van der Meulen, M.J., Buitter, S.J.H., Meulenkamp, J.E., Wortel, M.J.R., 2000. An early Pliocene uplift of the central Apenninic foredeep and its geodynamic implications. *Tectonics* 19, 300–313. DOI: 10.1029/1999TC900064.
- Wortel, M. J. R., Spakman, W., 2000. Subduction and slab detachment in the Mediterranean-Carpathian region. *Science* 290, 1910–1917. doi:10.1126/science.290.5498.1910.
- Wortel, R., Govers, R., Spakman, W., 2009. Continental collision and the STEP-wise evolution of convergent plate boundaries: From structure to dynamics. In Lallemand, S., Funiciello, F., (Eds.), *Subduction Zone Geodynamics*, Springer, Berlin, pp. 47–59. doi:10.1007/978-3-540-87974-9.
- Zhao, L.S., Helmberger, D., 1994. Source estimation from broad-band regional seismograms. *Bulletin of the Seismological Society of America* 85, 590–605.
- Zhu, L., Helmberger, D., 1996. Advancement in source estimation technique using broadband regional seismograms. *Bulletin of the Seismological Society of America* 86, 1634–1641.
- Zoback, M.L., 1992. First and second order patterns of stress in the lithosphere: the World Stress Map Project. *J. geophys. Res.* 97, 11 703–11 728.

FIGURE CAPTIONS

Figure 1 – Geodynamic setting of the study area represented by the yellow box. The geological model is modified from Morelli and Barrier (2004) and Polonia et al. (2011). In green GPS vectors in the Apulia fixed reference frame in which the motion of Calabria is parallel to the slip vector suggesting the existence of active crustal compression as a result of subduction of the Ionian lithosphere beneath the Calabrian Arc (D'Agostino et al., 2008). The NW ward dipping subducting

slab of the African plate is represented by the yellow isodepth lines in the Tyrrhenian Sea spacing from 100 to 450 km depth (Selvaggi and Chiarabba, 1995). ATL: Aeolian-Tindari-Letojanni fault.

Figure 2 – Structural map of the Calabrian Arc (CA) region derived from previous studies (modified from *Polonia et al.*, 2011), superposed over a grey levels bathymetric slope map. Major structural boundaries, active faults and the extent of the structural domains (i.e. pre and post-Messinian wedges and inner plateau) are indicated. Black thick lines correspond to the MCS data shown in Figure 3. The continental margin is segmented both across and along strike. The Alfeo-Etna fault system (AEF) and the splay faults (splay 1, 2 and 3) are considered active features likely to have generated major earthquakes in the past (Polonia et al., 2012). The IF is the diffuse structural boundary between EL and WL accommodating different rates of shortening, slab rollback and subduction dynamics in the different segments of the CA subduction zone.

Figure 3 – Line drawings of pre-stack depth migrated 36 fold MCS lines used for structural reconstructions. Location of seismic profiles is shown in Figure 2. (a) CROP M2B collected orthogonal to the continental margin in the WL from the Messina Straits region to the abyssal plain. In this region, the Post-Messinian accretionary complex detaches above the base of the Messinian evaporites. The well layered Tertiary and Mesozoic African plate sediments are attached to the lower plate and move towards NW. Splay faults form where the basal detachment cuts through deeper levels. (b) CROP line M4 collected in the EL of the Calabrian Arc subduction complex orthogonally to the main structural trends. Deformation in the outer wedge is related to the presence of duplex structures and an imbricate fan detaching on a deeper level within the basement. Structural style and basement involved tectonics suggest that this region is characterized by higher coupling, shortening and uplift rates. (c) CROP line M-3 across the transition between the Malta escarpment and CA accretionary wedge. At the toe of the Malta escarpment, the post-Messinian salt bearing complex lies on the basal detachment (top of Messinian evaporites) and is covered by a 800 m thick chaotic body representing a lower Pliocene olistostrome. At trace number 1×10^4 , a lithospheric-scale fault system is imaged, along which large offset vertical displacement of seismic reflectors is present and a fan shaped sedimentary basin develops.

Figure 4 – Location of geophysical data available in the working area (morphobathymetry from GEBCO database). Seismic data presented in this paper are indicated by thick red (Calamare dataset), yellow (ENI dataset), green (CROP dataset), blue (Sparker) and black (Chirp) lines.

Figure 5 – Time migrated 36 fold MCS line CROP M-31 (a) and its line-drawing (b). Location of seismic profile is shown in Figure 4. This profile has been collected in the Messina Straits region where a complex tectonic setting is outlined by oppositely dipping thrust sheets cut by a major sub-vertical fault system which re-activates pre-existing thrust faults.

Figure 6 – High resolution MCS time migrated seismic lines CA99-215 across the IF system in the region close to the Messina Straits (see Figure 4 for location).

Figure 7 – a: High resolution MCS time migrated seismic line CALA-02 across the WL at the transition between the Malta escarpment to the West and the accretionary wedge to the East (see Figure 4 for location). b: line drawing. Both AEF and IF control the formation of sedimentary basins filled by up to 800 m of sediments. The basement of the sedimentary basin between s.p. 300-800 is tilted along the IF system. c: Chirp seismic line collected close to MCS line CALA 02 (Figure 4 for

location). In this profile, the two opposite sets of normal faults are imaged on both sides of the sedimentary basin, which is filled by loose and coarse sand, which inhibited core recovery.

Figure 8 – Pre stack depth migrated MCS line CROP M-3 crossing orthogonally main transverse faults segmenting the subduction system. The seismic line crosses from West to East the Malta escarpment, the WL and EL of the accretionary wedge, which shows different basal detachment depths. The AEF bounds the transition from the salt bearing post-Messinian and the pre-Messinian clastic accretionary wedges in the WL where a sedimentary basin develops. The IF marks the boundary between the WL and EL and a diffuse area of deformation is observed with displacement of the deep units (i.e. Mesozoic carbonates and basement) accompanied by the formation of a series of ridges and troughs at the seafloor. Major tectono-stratigraphic units are represented by different colors.

Figure 9 – High resolution, single channel Sparker and Chirp profiles analyzed to address the fine geometry of single fault strands. Location of seismic lines is shown in Figure 4. a: Sparker seismic line across a fan shaped sedimentary basin developing above a major normal fault. This fault impinges along the coasts of Sicily north of the Mt. Etna. b: Chirp profile collected on the opposite side of the entrance of the Messina Straits across the IF system showing a set of two normal faults offsetting the seafloor and possibly triggering mass flow processes. c: Chirp seismic line collected across the IF system shows two oppositely dipping steep scarps along which the seafloor is downthrown of about 80 and 50 m. The zoom of the Chirp profile shows active deformation reaching the seafloor on the eastern fault block. d: Chirp profile across a fan shaped basin developing at the toe of the IF system suggesting syn-tectonic sedimentation. e: Chirp profile collected in the flat region at the toe of the IF system where a slope terrace develops. The zoom shows a wedging out pattern of the basin infill to the East suggesting syn-tectonic sedimentation. f: Chirp seismic line collected in the slope terrace at the toe of the IF system showing three fault scarps marked by roll-over anticlines along which sediments are progressively downthrown and deformed.

Figure 10 - Detailed structural map of the plate boundary region derived from this study which combines onland/offshore tectonics results over a bathymetric map collected during different cruises by the CIESM/IFREMER Medimap group (Loubrieu et al., 2008). Major structural boundaries, active faults and the extent of the structural domains (i.e. WL, EL, pre and post-Messinian wedges and inner plateau) are indicated. The continental margin is segmented along two major fault systems whose wide deformation zone is represented by the light blue pattern (i.e. Ionian fault system and Alfeo-Etna fault system). Horizontal velocities of continuous GPS stations and survey-mode GPS stations, with 95% confidence error ellipses, with respect to the Eurasian plate are modified from Figure 3 of Mastrolembo Ventura et al. (2014). Different arrow colors identify blocks with similar horizontal velocities: their boundaries are in good agreement with the location of AEF and IF and major faults onland. In red are marked major faults analyzed in this study while white faults represent regional structural features. White large arrows represent shortening along the outer deformation front (higher rates in the EL) of the subduction systems and extension in the WL. ATL: Aeolian-Tintari-Letojanni fault system.

Figure 11 – Bathymetric profiles (1 to 5) across the Ionian Fault system at the transition between the two lobes of the subduction complex.

Figure 12 – The plots 'a' to 'd' show the epicenter locations of the earthquakes of duration magnitude $M_d \geq 2.5$ occurring between 1997 and 2012 at different depths in southern Italy.

Numbers in low-right corners indicate depth-ranges in kilometres below sea level. The oblique box indicates the main study area of the present work. AEF and IF stand for Alfeo-Etna Fault System and Ionian Fault, respectively.

Figure 13 – Best quality focal mechanisms selected among waveform inversion solutions available for earthquakes occurring between 1977 and 2012 in the main study area of this work (section 'a'). Different colours correspond to different types of mechanisms according to the classification adopted in the World Stress Map (Zoback 1992; <http://dc-app3-14.gfz-potsdam.de/>): red = normal faulting (NF); orange = normal faulting with a minor strike-slip component (NS); green = strike-slip faulting (SS); blue = thrust faulting (TF); light-blue = thrust faulting with a minor strike-slip component (TS); black = unknown stress regime (U). The beach ball size is proportional to the earthquake magnitude. Numbering refers to earthquake ID numbers of Table 2. Section 'b' reports the polar plots of P- and T-axes (full and empty dots, respectively) relative to the whole set of focal mechanisms of Section 'a' (left), the Alfeo-Etna Fault System zone (center) and the Ionian Fault zone (right). Section 'c' shows a NW-SE oriented vertical section (see the dashed black line in section 'a' for the profile) including the focal mechanism solutions of earthquakes located around the Ionian Fault (marked with an asterisk in Table 2) and the reconstruction of upper/lower plate velocity structure taken from Neri et al. (2012).

Figure 14 - Results of our mechanical models where strain localization ahead of the active STEP indicates its propagation direction. Thick black lines represent approximate outlines of continental blocks in reconstructed positions at Time 1 (approximately Early-Middle Pliocene), Time 2 (~ Pleistocene) and Time 3 (Present). Thinner and double (train track like) black lines outline the approximate passive margin. Red lines represent faults that are active within the given time frames (solid lines are STEP faults, dashed line is Malta Escarpment), and colored balls indicate fault slip rates. The orange wedge in the panels at Time 2 and 3 show the range of orientations in which the STEP could have migrated since then: pre-existing weak and near-vertical faults with strike orientations within this wedge would have been re-activated. If such faults did not exist, a new vertical shear/fault zone would be initiated along the maximum shear strain direction. See text for further explanation.

Figure 15 – Schematic representation of the geodynamic context of the Sicily-Calabria region. Two principal lithospheric scale components are represented: 1) the relative motion of the African and Eurasian plates, and 2) the retreat of the Calabrian slab. The convergent plate boundary ESE of Calabria refers to the boundary at the basement level, below the accretionary wedge (Figure 3b). The boundary's orientation and SW end are based on seismic tomography (e.g. Giacomuzzi et al., 2012) and the distribution of earthquake hypocentres in the subducting Calabrian slab (Selvaggi and Chiarabba, 1995; see also isodepth lines in Figure 1). GPS-velocity directions of Eurasia relative to Africa and of the migrating Calabrian Arc relative to Africa are after d'Agostino et al. (2008). The dashed line indicates the regional Africa-Eurasia plate boundary; the westernmost segment (in magenta) accommodates convergence, whereas to the east of it the plate boundary shows strike-slip motion (Billi et al., 2006, 2007, 2011). The hatched zone indicates the dextral shear zone resulting from the resistance encountered in the eastern part of the plate boundary in the southern Tyrrhenian Sea. The Alfeo-Etna Fault (AEF, marked light brown) is part of this shear zone. The NW part (marked yellow) of the Ionian Fault (IF) is the surface expression corresponding with the slab edge related STEP activity in the basement. The inset (lower left, modified after Forsyth

(1975)) schematically shows the deformation, involving downflexing of the lithosphere, in front of the tip of a propagating tear fault (STEP).

TABLE CAPTIONS

Table 1 - Acquisition parameters, processing sequence and resolution of geophysical data used in this study

Table 2 - Main parameters of focal mechanisms reported in Fig. 13. ID is the order number (same as in Fig. 13). Mw is the moment magnitude. FT is faulting type according to Zoback's (1992) definition: NF=normal faulting, NS=normal faulting with a minor strike-slip component, SS=strike-slip faulting, TF=thrust faulting, TS=thrust faulting with a minor strike-slip component, and U=unknown stress regime. ID numbers marked with asterisks indicate the focal mechanisms reported in Fig.13c. The sources of data are the Italian Centroid Moment Tensor catalogue (ItCMT), the paper by Orecchio et al. (2014), and the present work.

Table 3 - Mechanical model parameters

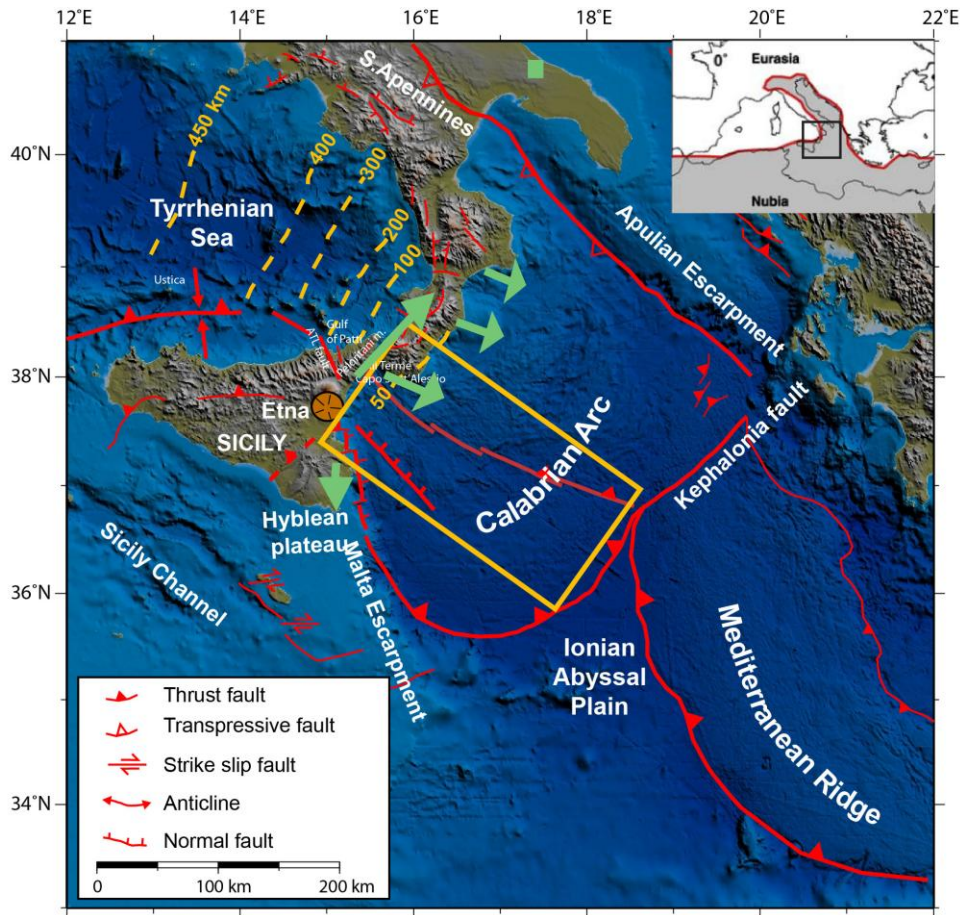


Figure 1 – Geodynamic setting of the study area represented by the yellow box. The geological model is modified from Morelli and Barrier (2004) and Polonia et al., (2011). In green GPS vectors in the Apulia fixed reference frame in which the motion of Calabria is parallel to the slip vector suggesting the existence of active crustal compression as a result of subduction of the Ionian lithosphere beneath the Calabrian Arc (D’Agostino et al., 2008). The NW ward dipping subducting slab of the African plate is represented by the yellow isodepth lines in the Tyrrhenian Sea spacing from 100 to 450 Km depth (Selvaggi and Chiarabba, 1995). ATL: Aeolian-Tindari-Letojanni fault.

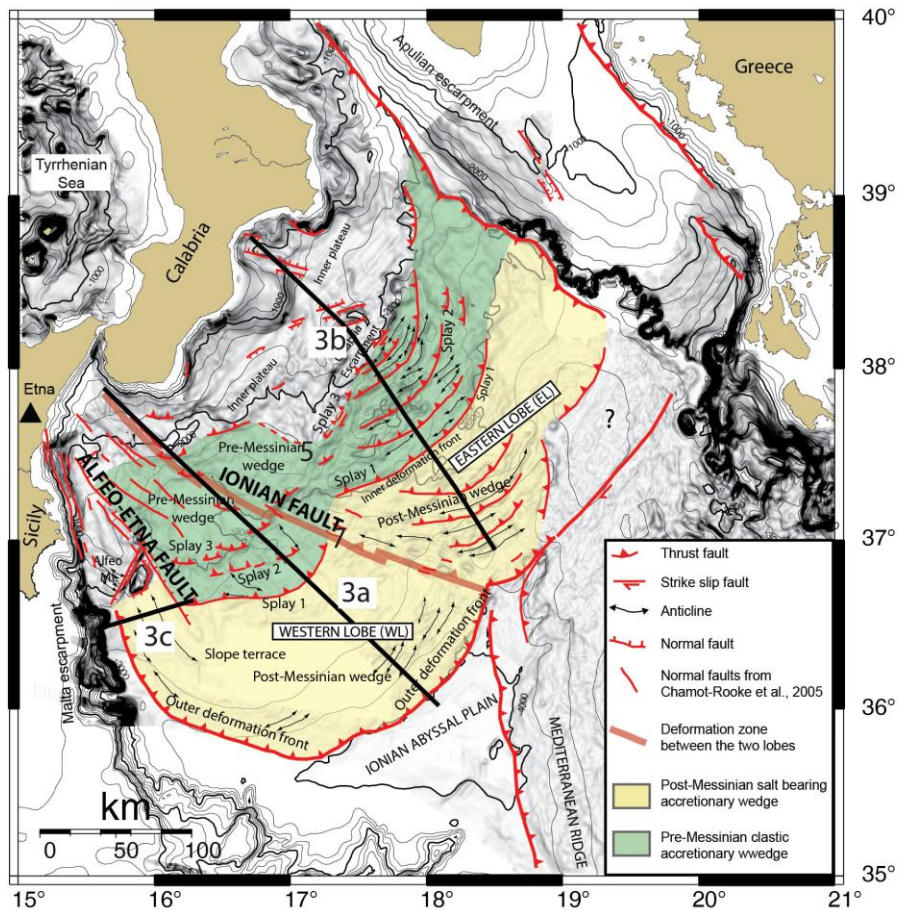


Figure 2 – Structural map of the Calabrian Arc (CA) region derived from previous studies (modified from *Polonia et al., 2011*), superposed over a grey levels bathymetric slope map. Major structural boundaries, active faults and the extent of the structural domains (i.e. pre and post-Messinian wedges and inner plateau) are indicated. Black thick lines correspond to the MCS data shown in Figure 3. The continental margin is segmented both across and along strike. The Alfeo-Etna fault system (AEF) and the splay faults (splay 1, 2 and 3) are considered active features likely to have generated major earthquakes in the past (*Polonia et al., 2012*). The IF is the diffuse structural boundary between EL and WL accommodating different rates of shortening, slab rollback and subduction dynamics in the different segments of the CA subduction zone.

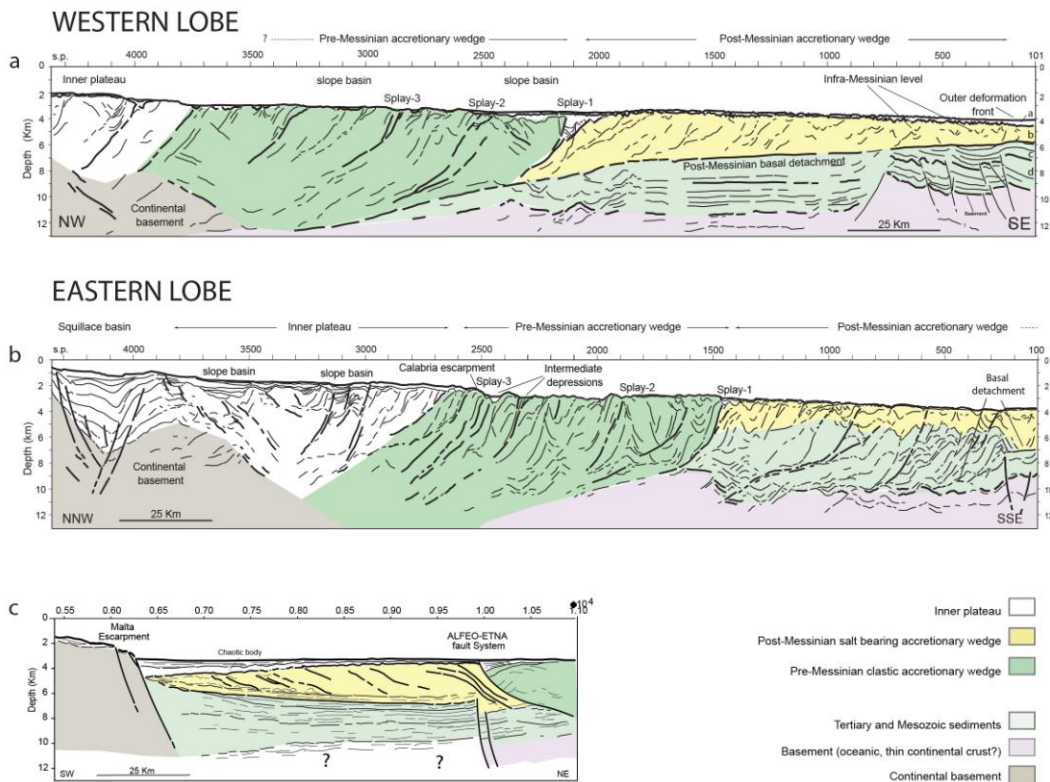


Figure 3 – Line drawings of pre-stack depth migrated 36 fold MCS lines used for structural reconstructions. Location of seismic profiles is shown in Figure 2. (a) CROP M2B collected orthogonal to the continental margin in the WL from the Messina Straits region to the abyssal plain. In this region, the Post-Messinian accretionary complex detaches above the base of the Messinian evaporites. The well layered Tertiary and Mesozoic African plate sediments are attached to the lower plate and move towards NW. Splay faults form where the basal detachment cuts through deeper levels. (b) CROP line M4 collected in the EL of the Calabrian Arc subduction complex orthogonal to the main structural trends. Deformation in the outer wedge is related to the presence of duplex structures and an imbricate fan detaching on a deeper level within the basement. Structural style and basement involved tectonics suggest that this region is characterized by higher coupling, shortening and uplift rates. (c) CROP line M-3 across the transition between the Malta escarpment and CA accretionary wedge. At the toe of the Malta escarpment, the post-Messinian salt bearing complex lies on the basal detachment (top of Messinian evaporites) and is covered by a 800 m thick chaotic body representing a lower Pliocene olistostrome. At trace number 1×10^4 , a lithospheric-scale fault system is imaged, along which, large offset vertical displacement of seismic reflectors is present and a fan shaped sedimentary basin develops.

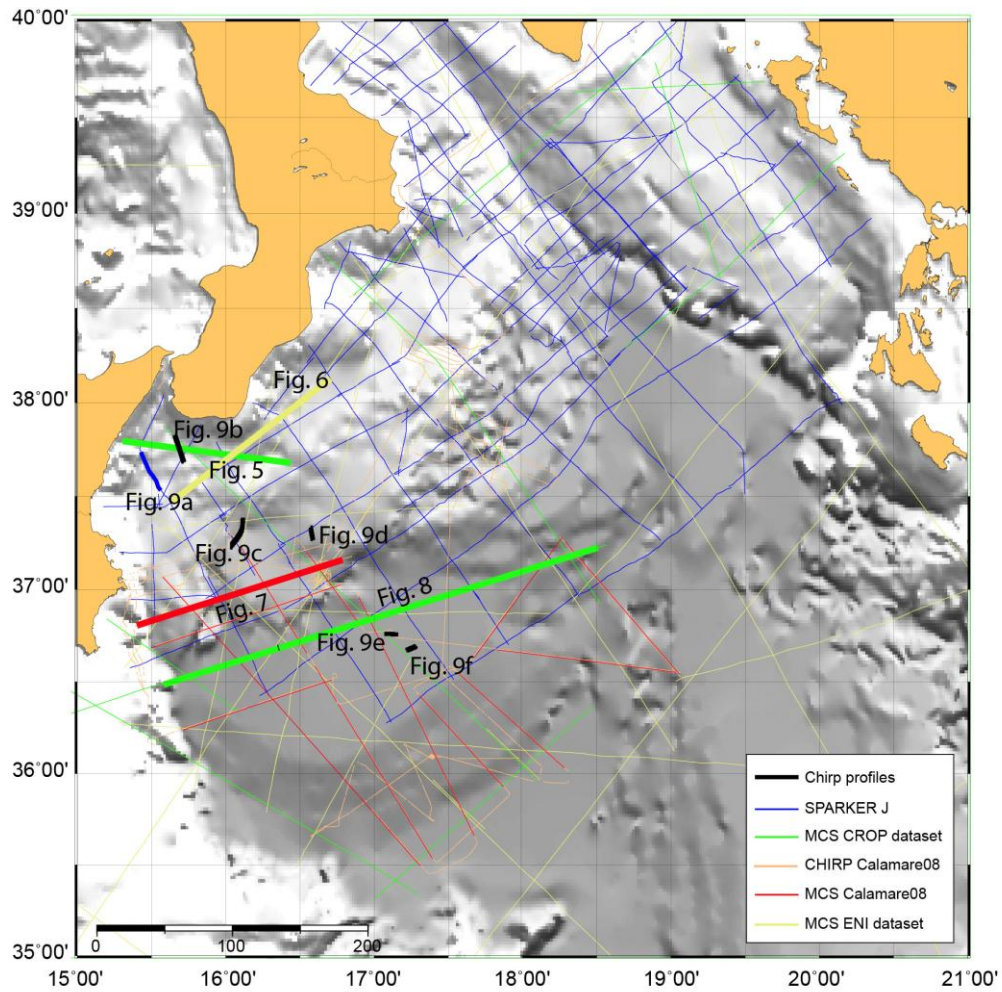


Figure 4 – Location of geophysical data available in the working area (morphobathymetry from GEBCO database). Seismic data presented in this paper are indicated by thick red (Calamare dataset), yellow (ENI dataset), green (CROP dataset), blue (Sparker) and black (Chirp) lines.

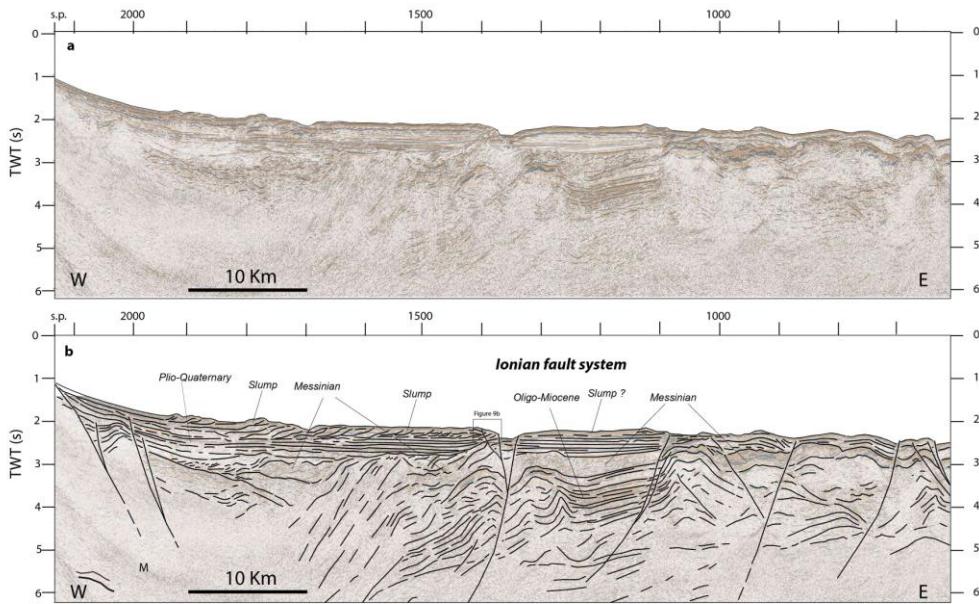


Figure 5 – Time migrated 36 fold MCS line CROP M-31 (a) and its line-drawing (b). Location of seismic profile is shown in Figure 4. This profile has been collected in the Messina Straits region where a complex tectonic setting is outlined by opposite dipping thrust sheets cut by a major sub-vertical fault system which re-activates pre-existing thrust faults.

ACCEPTED

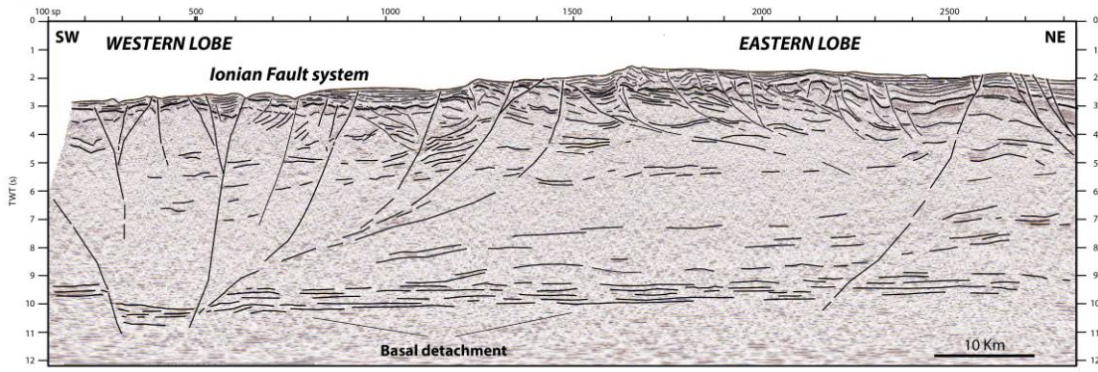


Figure 6 – High resolution MCS time migrated seismic lines CA99-215 across the IF system in the region close to the Messina Straits (see Figure 4 for location).

ACCEPTED MANUSCRIPT

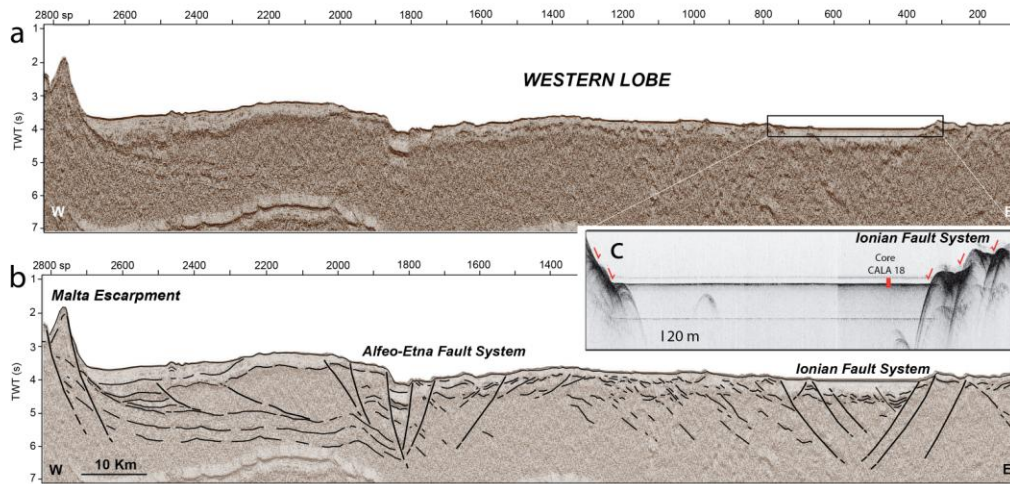


Figure 7 – a: High resolution MCS time migrated seismic line CALA-02 across the WL at the transition between the Malta escarpment to the West and the accretionary wedge to the East (see Figure 4 for location). b: line drawing. Both AEF and IF control the formation of sedimentary basins filled by up to 800 m of sediments. The basement of the sedimentary basin between s.p. 300-800 is tilted along the IF system. c: Chirp seismic line collected close to MCS line CALA 02 (Figure 4 for location). In this profile, the two opposite set of normal faults are imaged on both sides of the sedimentary basin, which is filled by loose and coarse sand, which inhibited core recovery.

ACCEPTED

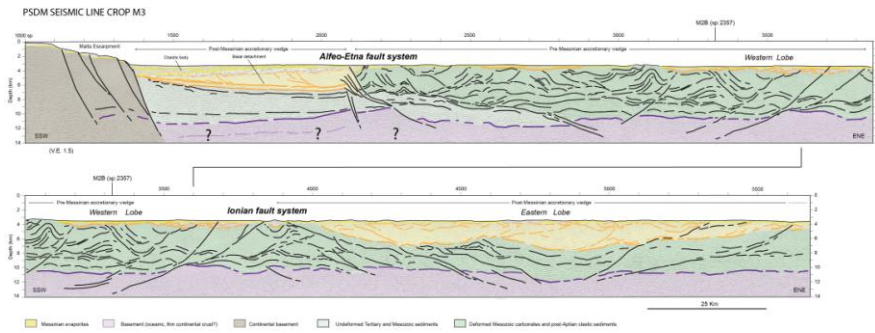


Figure 8 – Pre stack depth migrated MCS line CROP M-3 crossing orthogonally main transverse faults segmenting the subduction system. The seismic line crosses from West to East the Malla escarpment, the WL and EL of the accretionary wedge, which shows different basal detachment depths. The AEF bounds the transition from the salt bearing post-Messinian and the pre-Messinian clastic accretionary wedges in the WL where a sedimentary basin develops. The F marks the boundary between the WL and EL and a diffuse area of deformation is observed with displacement of the deep units (i.e. Mesozoic carbonates and basement) accompanied by the formation of a series of ridges and troughs at the seafloor. Major tectono-stratigraphic units are represented by different colors.

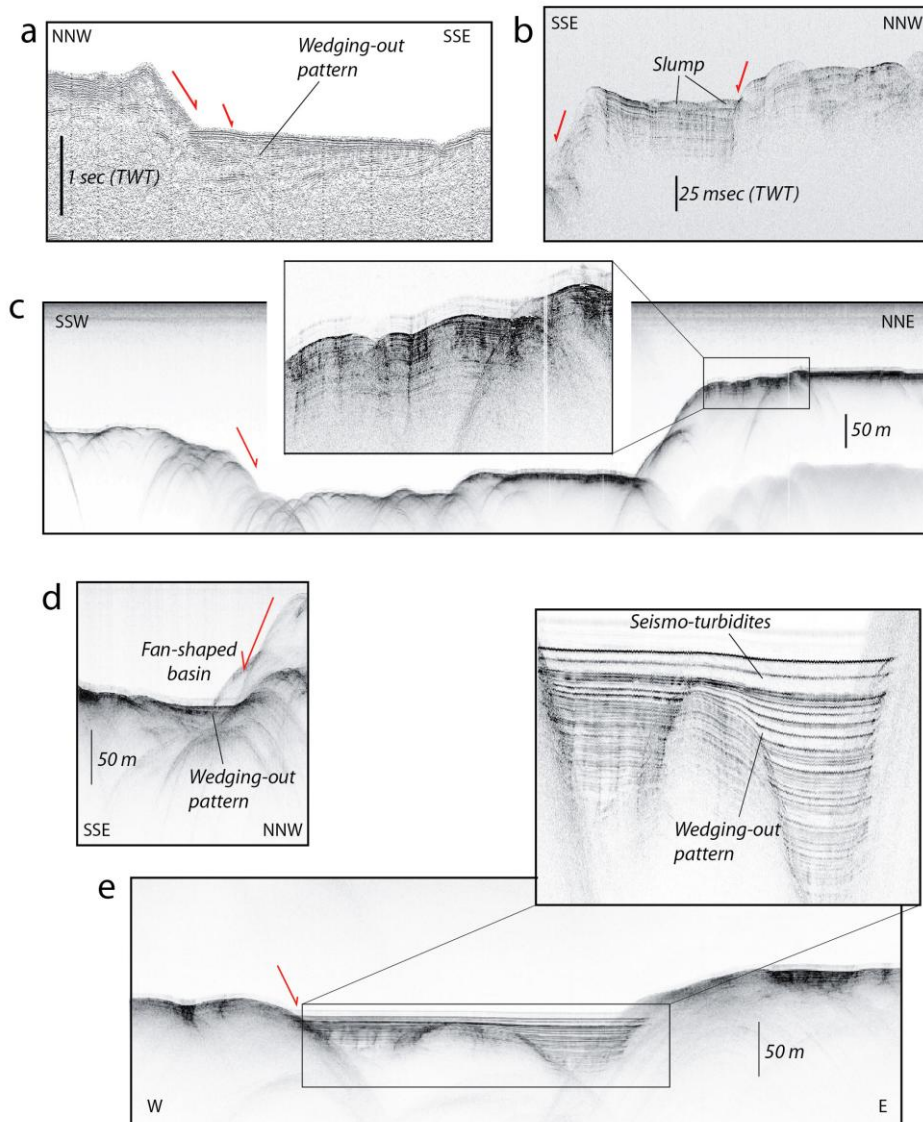


Figure 9 – High resolution, single channel Sparker and Chirp profiles analyzed to address the fine geometry of single fault strands. Location of seismic lines is shown in Figure 4. a: Sparker seismic line across a fan shaped sedimentary basin developing above a major normal fault. This fault impinges along the coasts of Sicily north of the Mt. Etna. b: Chirp profile collected on the opposite side of the entrance of the Messina Straits across the IF system showing a set of two normal faults offsetting the seafloor and possibly triggering mass flow processes. c: Chirp seismic line collected across the IF system shows two opposite dipping steep scarps along which the seafloor is downthrown of about 80 and 50 m. The zoom of the Chirp profile shows active deformation reaching the seafloor on the eastern fault block. d: Chirp profile across a fan shaped basin developing at the toe of the IF system suggesting syn-tectonic sedimentation. e: Chirp profile collected in the flat region at the toe of the IF system where a slope terrace develops. The zoom shows a wedging out pattern of the basin infill to the East suggesting syn-tectonic sedimentation. f: Chirp seismic line collected in the slope terrace at the toe of the IF system showing three fault scarps marked by roll-over anticlines along which sediments are progressively downthrown and deformed.

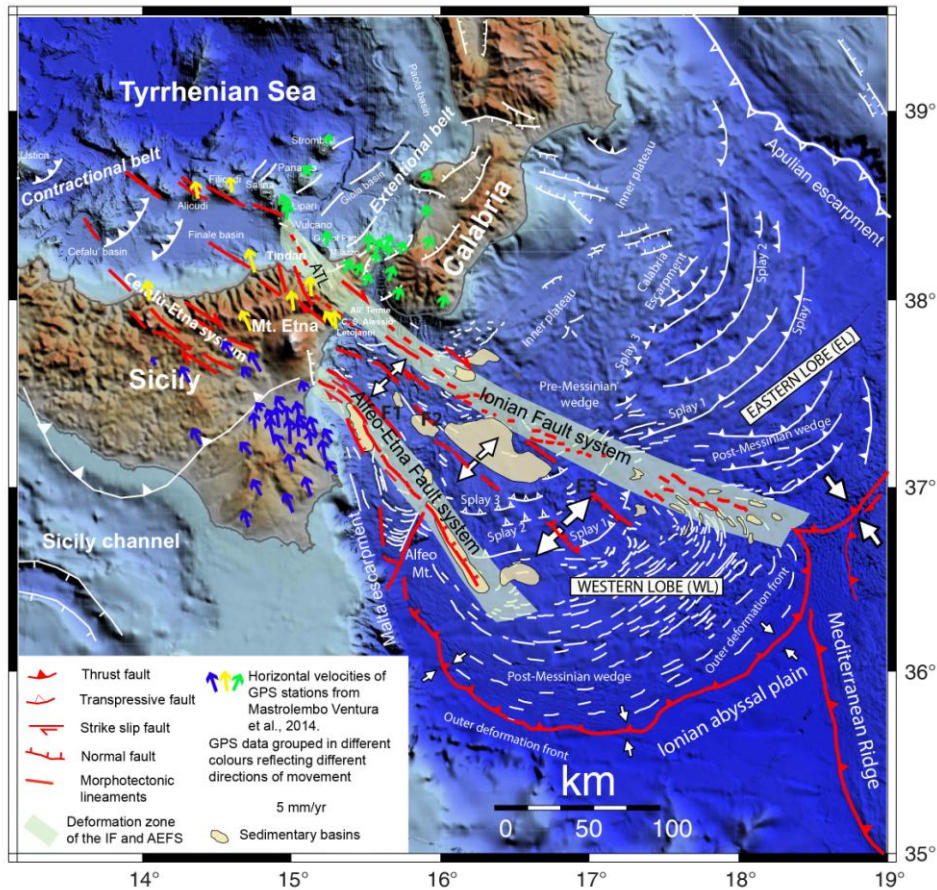


Figure 10 - Detailed structural map of the plate boundary region derived from this study which combines onland/offshore tectonics results over a bathymetric map collected during different cruises by the CIESM/IFREMER Medimap group (Loubrieu et al., 2008). Major structural boundaries, active faults and the extent of the structural domains (i.e. WL, EL, pre and post-Messinian wedges and inner plateau) are indicated. The continental margin is segmented along two major fault systems whose wide deformation zone is represented by the light blue pattern (i.e. Ionian fault system and Alfeo-Etna fault system). Horizontal velocities of continuous GPS stations and survey-mode GPS stations, with 95% confidence error ellipses, with respect to the Eurasian plate are modified from Figure 3 of Mastrolembo Ventura et al. (2014). Different arrow colors identify blocks with similar horizontal velocities: their boundaries are in good agreement with the location of AEF and IF and major faults onland. In red are marked major faults analyzed in this study while white faults represent regional structural features. White large arrows represent shortening along the outer deformation front (higher rates in the EL) of the subduction systems and extension in the WL. ATL: Aeolian-Tintari-Letojanni fault system.

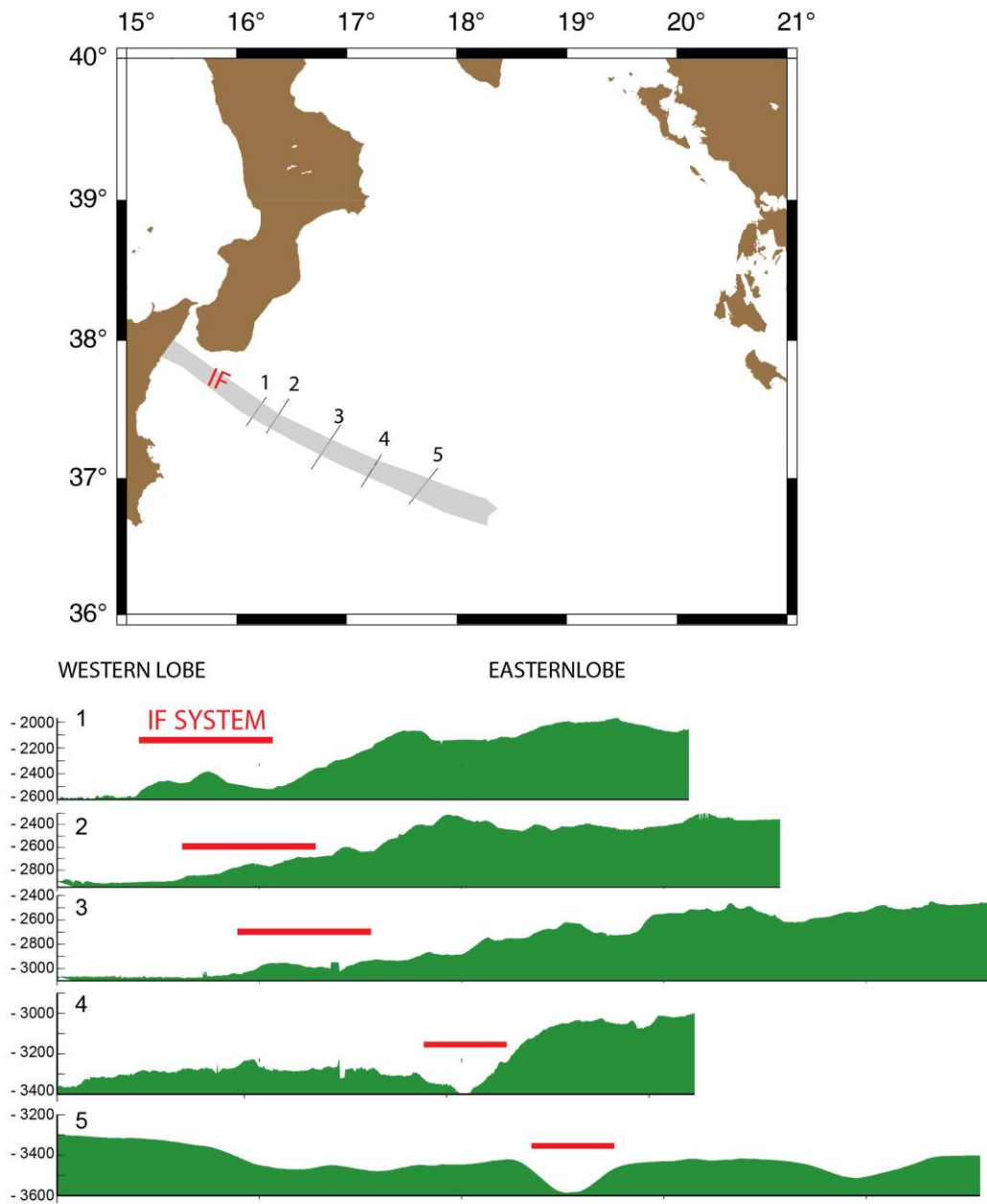


Figure 11 – Bathymetric profiles (1 to 5) across the Ionian Fault system at the transition between the two lobes of the subduction complex.

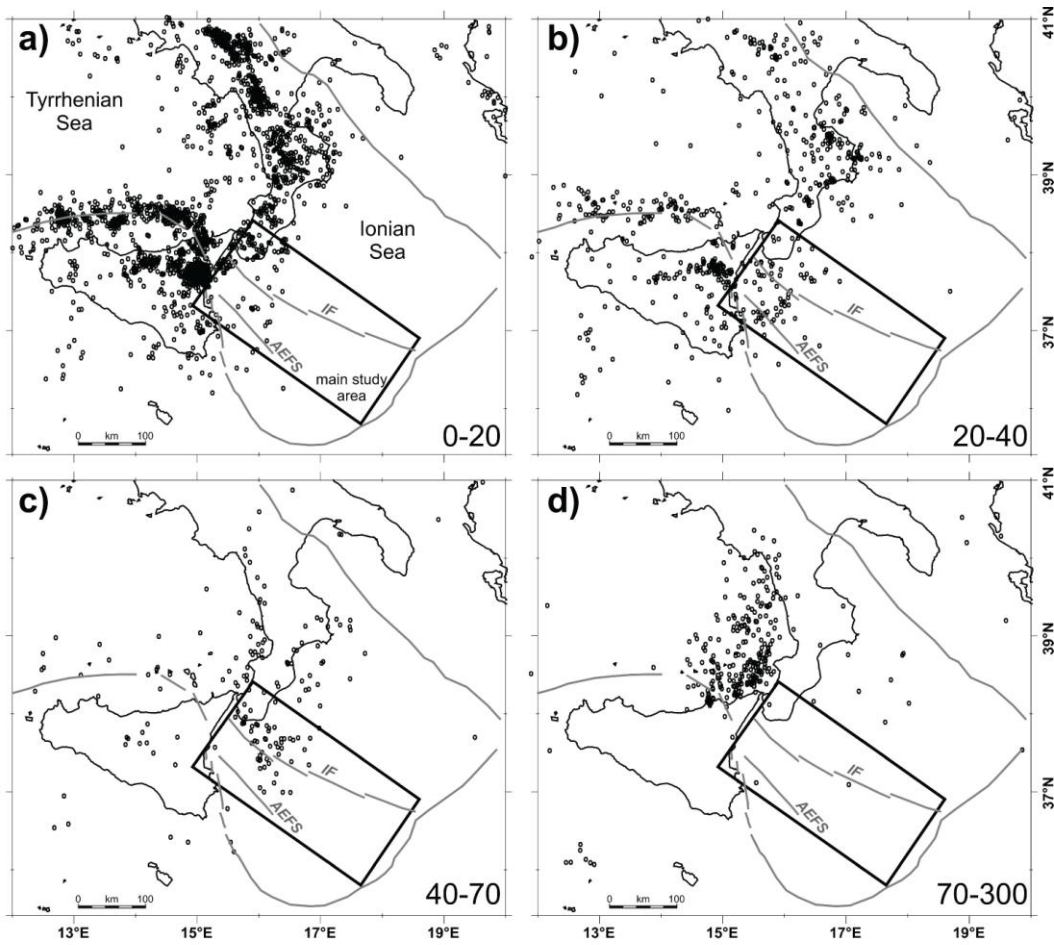


Figure 12 – The plots 'a' to 'd' show the epicenter locations of the earthquakes of duration magnitude $M_d \geq 2.5$ occurring between 1997 and 2012 at different depths in southern Italy. Numbers in low-right corners indicate depth-ranges in kilometres below sea level. The oblique box indicates the main study area of the present work. AEF and IF stand for Alfeo-Etna Fault System and Ionian Fault, respectively.

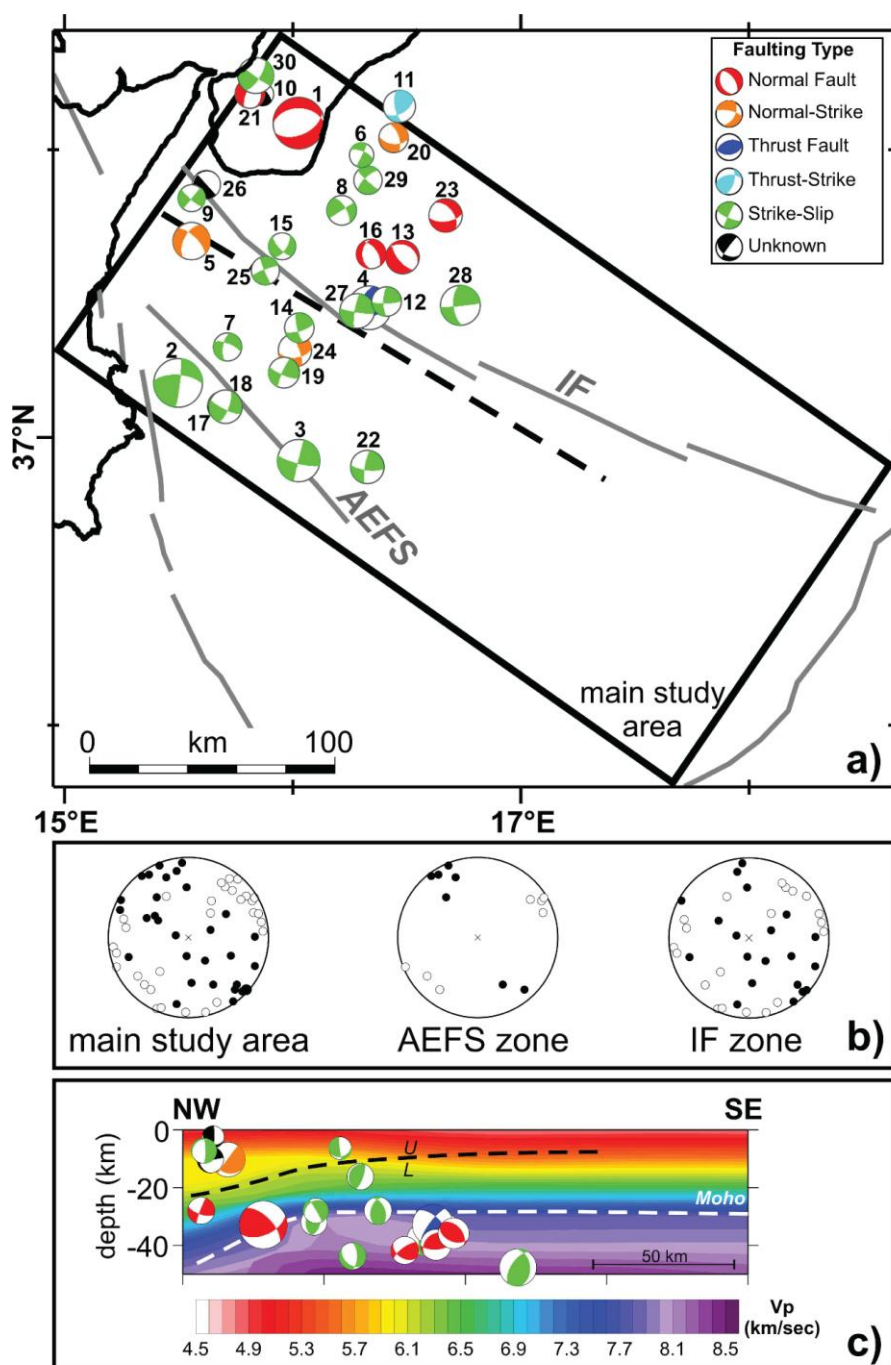


Figure 13 – Best quality focal mechanisms selected among waveform inversion solutions available for earthquakes occurring between 1977 and 2012 in the main study area of this work (section ‘a’). Different colours correspond to different types of mechanisms according to the classification adopted in the World Stress Map (Zoback 1992; <http://dc-app3-14.gfz-potsdam.de/>): red = normal faulting (NF); orange = normal faulting with a minor strike-slip component (NS); green = strike-slip faulting (SS); blue = thrust faulting (TF); light-blue = thrust faulting with a minor strike-slip component (TS); black = unknown stress regime (U). The beach ball size is proportional to the earthquake magnitude. Numbering refers to earthquake ID numbers of Table 2. Section ‘b’ reports the polar plots of P- and T-axes (full and empty dots, respectively) relative to the whole set of focal mechanisms of Section ‘a’ (left), the Alfeo-Etna Fault System zone (center) and the Ionian Fault zone (right). Section ‘c’ shows a NW-SE oriented vertical section (see the dashed black line in section ‘a’ for the profile) including the focal mechanism solutions of earthquakes located around the Ionian Fault (marked with an asterisk in Table 2) and the reconstruction of upper/lower plate velocity structure taken from Neri et al. (2012).

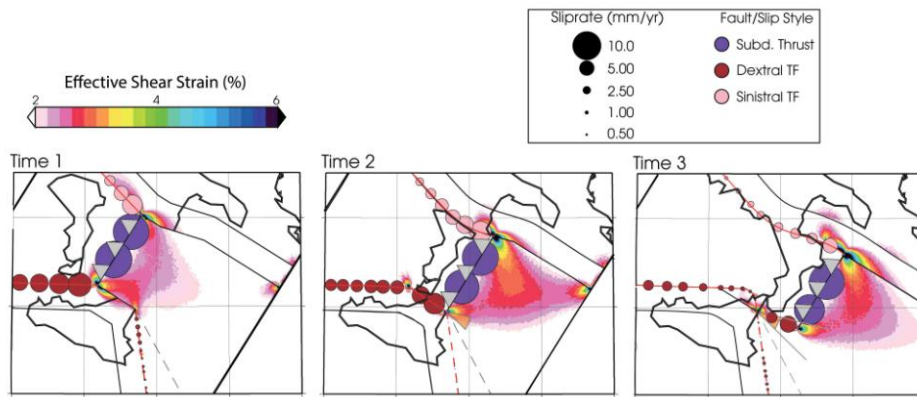


Figure 14 - Results of our mechanical models where strain localization ahead of the active STEP indicates its propagation direction. Thick black lines represent approximate outlines of continental blocks in reconstructed positions at Time 1 (approximately Early-Middle Pliocene), Time 2 (~ Pleistocene) and Time 3 (Present). Thinner and double (train track like) black lines outline the approximate passive margin. Red lines represent faults that are active within the given time frames (solid lines are STEP faults, dashed line is Malta Escarpment), and colored balls indicate fault slip rates. The orange wedge in the panels at Time 2 and 3 show the range of orientations in which the STEP could have migrated since then: pre-existing weak and near-vertical faults with strike orientations within this wedge would have been re-activated. If such faults did not exist, a new vertical shear/fault zone would be initiated along the maximum shear strain direction. See text for further explanation.

ACCEPTED MANUSCRIPT

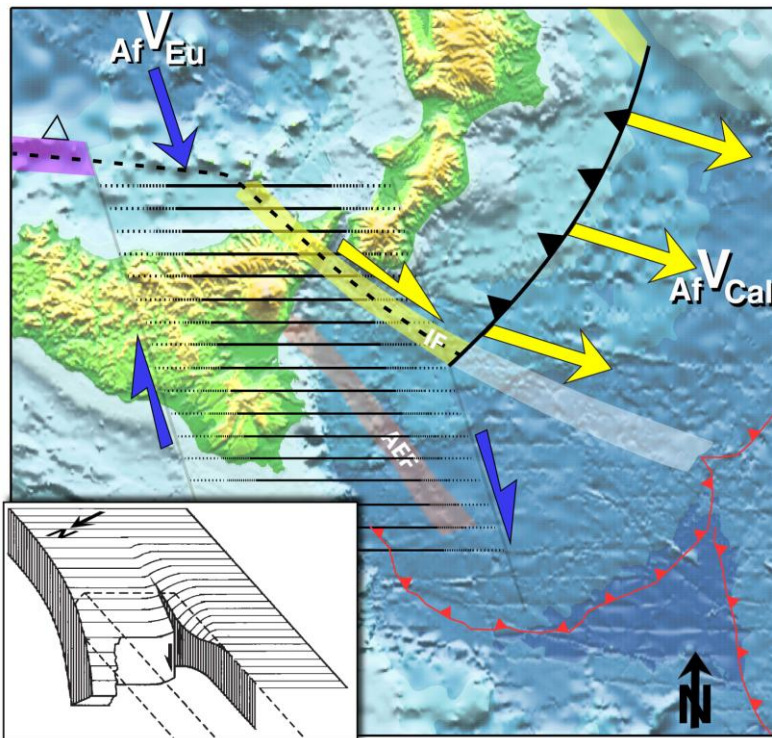


Fig. 15

GEOPHYSICAL MULTI-SCALE DATASET	Acquisition parameters	Main processing sequence	Resolution in space
CROP MCS dataset	Source: 4906 cu inch air guns Streamer: 4500 m Group interval: 25 m Shot Interval: 62.5 m Coverage: 3600% Sampl. Int.: 4 msec	Full pre-stack depth-migration (PSDM), with SIRIUS/GXT, Migpack software package.	km-scale
ENI CA MCS	Source: 3400 cu inch air guns Streamer: 6200 m Group interval: 12.5 m Shot Interval: 25.0 m Coverage: 12000% Sampl. Int.: 2 msec	Velocity analysis, stack, migration	nX100 to km scale
CALAMARE MCS dataset	Source: 2 Soderia G.I. guns, Streamer: 600 m Group int.: 12.5 m Shot interval: 50 m Coverage: 600% Sampl. Int.: 1 msec	Velocity analysis, stack, DMO, velocity analysis, stack, migration	nx100 m to km scale
Sparker seismic data	Source: 30 kJ Teledyne system Streamer: active section: 50 m, single channel Shot Interval: 4-8 sec (12-24 m)		
Chirp dataset	17 hull mounted 17 transducers CHIRP-Benthos sonar system (3-7 KHz sweep frequency)	Data represented through variable density sections with instantaneous amplitude	Metric/decimetric
Multibeam data (IFREMER, MEDIMAP group, Loubrieu et al., 2008)	Simrad EM-300	500 m grid provided by the MEDIMAP group	500 m grid

Table 1 – Acquisition parameters, processing sequence and resolution of geophysical data used in this study

Key Points (must be complete thoughts, under 80 characters)

- 1) Plate boundary re-organization in the central Mediterranean Sea
- 2) Segmentation of the subduction complex along lithospheric transverse faults
- 3) STEP faults in the Ionian Sea
- 4) Pleistocene active faulting and Mt. Etna formation